

Proper Dataset Valuation by Pointwise Mutual Information

Shuran Zheng*

shuranzheng@mail.tsinghua.edu.cn
Tsinghua University

Xuan Qi*

qi-x22@mails.tsinghua.edu.cn
Tsinghua University

Rui Ray Chen*

chenrui20@mails.tsinghua.edu.cn
Tsinghua University

Yongchan Kwon

yk3012@columbia.edu
Columbia University

James Zou

jamesz@stanford.edu
Stanford University

Abstract

Data plays a central role in advancements in modern artificial intelligence, with high-quality data emerging as a key driver of model performance. This has prompted the development of principled and effective data curation methods in recent years. However, existing methods largely rely on heuristics, and whether they are truly effective remains unclear. For instance, standard evaluation methods that assess a trained model’s performance on specific benchmarks may incentivize assigning high scores to data that merely resembles the test set. This issue exemplifies Goodhart’s law: when a measure becomes a target, it ceases to be a good measure. To address this issue, we propose an information-theoretic framework for evaluating data curation methods. We define dataset quality in terms of its informativeness about the true model parameters, formalized using the *Blackwell ordering of informativeness*. Under this ordering, Blackwell’s theorem ensures that more informative data yields optimal models with lower expected loss on the true underlying distribution. To measure informativeness, we show that the Blackwell order can be determined by the Shannon mutual information between the curated data and the test data. To estimate this mutual information, we introduce a novel method that trains Bayesian models on embedded datasets and computes mutual information from the posteriors of model parameters. Experiments on real-world data demonstrate that our mutual information-based evaluation assigns appropriately lower scores to data curation strategies that reduce dataset informativeness, while traditional test score-based evaluation methods may favor data curation strategies that overfit to the test set but compromise the training data’s informativeness.

*Equal contribution; names are listed in order of joining.

1 Introduction

Data plays a central role in the development of modern artificial intelligence (AI) systems, where the large volume and high quality of the data used in training are critical to model performance [Brown et al., 2020, Peebles and Xie, 2023, Team et al., 2024, Grattafiori et al., 2024]. As AI systems continue to grow larger and the computational costs of training escalate, the focus is shifting from simply expanding model and dataset sizes to enhancing the quality of the data itself. This shift has prompted the development of various data curation strategies, including data filtering [Gunasekar et al., 2023, Li et al., 2023, Fang et al., 2023, Pouget et al., 2024], duplicate removal [Kandpal et al., 2022], data augmentation [Muennighoff et al., 2024], and synthetic data generation [Liu et al., 2024].

However, ensuring the effectiveness of these curation techniques remains a major challenge [Li et al., 2024, Weber et al., 2024]. The standard evaluation approach involves training a model on a curated dataset and measuring its performance against benchmark test sets [Li et al., 2024, Albalak et al., 2024, Team et al., 2024, Grattafiori et al., 2024]. This methodology, though common, can inadvertently encourage undesirable curation practices that optimize performance on specific benchmarks, yet risk overfitting to the test data and undermining the model’s ability to generalize to new data. For instance, as noted by [Pouget et al., 2024], popular pre-training methods often filter datasets to emphasize English-language image-text pairs in order to maximize performance on western-oriented benchmarks like ImageNet and COCO. While this may improve performance on those benchmarks, it degrades performance on global datasets. This illustrates a critical issue: as highlighted by Goodhart’s law, when a measure becomes a target, it ceases to be a good measure.

An important question, therefore, is how to distinguish data curation methods that merely manipulate data to boost model performance on specific benchmarks from those that truly contribute meaningful data to the learning process. In this work, we propose an alternative information-theoretic framework that may help make this distinction: rather than measuring the test score of a trained model on specific test sets, we evaluate the *informativeness* of a dataset for a given machine learning task. To achieve this, we adopt the well-known Blackwell ordering [Blackwell et al., 1951] to compare the informativeness of datasets. Under this ordering, Blackwell’s theorem ensures that more informative data yields optimal models with lower expected loss on the true underlying distribution. Therefore, a data curation method is considered effective if it increases the dataset’s informativeness about the true model parameters, while it is deemed *strategic* if it decreases the dataset’s informativeness, according to the Blackwell ordering.

To quantify informativeness, we propose using the *Shannon mutual information* (MI) of the curated dataset and the test dataset as a metric. We show that MI effectively identifies data curation methods that truly reduce informativeness. Specifically, if a curation method decreases the dataset’s informativeness according to the Blackwell ordering, it must lead to a decrease in the mutual information. However, estimating the mutual information of two

datasets introduces a new challenge. Prior work on high-dimensional mutual information estimation has primarily focused on pairs of individual data points with dimensionality on the order of thousands (e.g., correlated image pairs from MNIST or CIFAR-10), but not on dataset pairs containing many such points.¹ To overcome this challenge, we propose a novel method for estimating the mutual information of two datasets. We exploit a dataset’s capacity to train a machine learning model and compute the mutual information using the posterior distributions of model parameters obtained from Bayesian models.

We demonstrate the effectiveness of our method through experiments on real-world datasets, including MNIST and CIFAR. First, we show that our MI estimator yields much more accurate estimates than previous methods, with theoretical support from a faster convergence rate that is independent of input dimensionality. Next, we show that the test score-based evaluation method may favor data curation strategies that make the dataset more similar to the test data but reduce its informativeness about the true model parameters. In contrast, our mutual information-based evaluation assigns appropriately lower scores to such strategies.

2 Related Work

Data curation. Due to the growing importance of data quality, recent years have seen a surge in diverse data curation techniques. Data filtering [Gunasekar et al., 2023, Li et al., 2023, Fang et al., 2023, Pouget et al., 2024, Xie et al., 2023] aims to select data points to include in the training dataset from a large pool of raw data, often guided by various heuristics. Duplicate removal [Kandpal et al., 2022] focuses on repeated occurrences and the impact of sequences within training datasets. The findings underscore the importance of sequence-level deduplication in training efficiency and model privacy without sacrificing model performance. Data augmentation [Muennighoff et al., 2024] generates new training samples from the original dataset to enhance its diversity and volume while preserving its core characteristics, while synthetic data generation [Liu et al., 2024] creates new data that closely resemble the distribution of real data. Data mixing [Xie et al., 2024, Liu et al., 2025] determines the weight of each domain’s dataset to optimize performance across all domains. Data distillation [Sachdeva and McAuley, 2023] aims to create compact, high-fidelity data summaries that capture the most essential knowledge from a given target dataset. MeCo [Gao et al., 2025] optimizes the data curation process by injecting additional metadata into the data, further refining its utility in model training. [Wettig et al., 2025] introduces the WebOrganizer framework, which classifies data based on both topics and formats before applying mixing optimization, thereby effectively enhancing the quality of pretraining data.

¹Gowri et al. [2024] show that existing neural estimators typically handle only tens of *intrinsic dimensions*. This is especially problematic, as datasets are inherently high-dimensional due to the large number of data points they contain. Given that the intrinsic dimensionality of images ranges from 20 to 43, as reported by Pope et al. [2021], existing methods may not be reliable when applied to datasets with just a few images.

For a more comprehensive survey of related work in this area, we refer readers to [Wettig et al., 2024].

Dataset valuation. Various methods have been proposed for dataset evaluation. The standard approach involves training a model on a curated dataset and measuring its performance on benchmark test sets [Li et al., 2024, Albalak et al., 2024]. Garrido-Lucero et al. [2024] leverage estimated Shapley values for efficient dataset valuation. Mohammadi Amiri et al. [2023] focus on intrinsic, task-agnostic dataset valuation by estimating data diversity and relevance without requiring a validation set. However, none of these methods provide the information-theoretic guarantees as we do. [Sim et al., 2020] evaluates the contribution of datasets by the mutual information of the model parameter and the data; however, their method does not detect strategic data curation methods. See Appendix B for related discussion.

Data point valuation. Besides dataset evaluation, the assessment of data point value has been actively studied in the data valuation literature. A standard approach is to measure the change in the test accuracy after removing a single training data point of interest. Data Shapley by Ghorbani and Zou [2019] deploys the Shapley value from cooperative game theory to ML settings, and several variants that improve its computational efficiency or relax underlying conditions have been proposed [Jia et al., 2019a, Kwon and Zou, 2021, Wang and Jia, 2022, Wang et al., 2024b, Pham et al., 2025, Wang et al., 2025, 2024a]. An alternative common approach utilizes the influence function introduced in robust statistics [Koh and Liang, 2017, Feldman and Zhang, 2020]. This method provides a mathematically rigorous interpretation of data values and has been implemented in various applications, such as image classification and sentiment analysis, or text-to-image generation [Park et al., 2023, Kwon et al., 2023]. [Wang et al., 2024c] efficiently captures temporal data influence in training while [Wang et al., 2024d] optimizes LLM training via Taylor-based batch selection. Other algorithm-agnostic and task-agnostic methods have also been explored, such as [Just et al., 2023, Xu et al., 2021, Lin et al., 2025]. There are also some theoretical works, Wang et al. [2024e] critically analyze Data Shapley’s limitations in selection tasks while Lin et al. [2024] introduce model deviation and NTK theory for validation-free robustness. We refer the readers to [Jiang et al., 2023] for a comprehensive and detailed review.

Peer prediction approach. Our method is also connected to the *peer prediction* literature [Miller et al., 2005, Prelec, 2004, Jurca and Faltungs, 2008, Radanovic and Faltungs, 2013, 2014, Witkowski and Parkes, 2012, Kong and Schoenebeck, 2018a, Schoenebeck and Yu, 2020b], which studies eliciting truthful information without ground truth. Among these, [Kong and Schoenebeck, 2018b, Chen et al., 2020b, Schoenebeck and Yu, 2020a] are most relevant. Kong and Schoenebeck [2018b] propose a mutual information-based peer prediction method using two agents’ predictions about a latent label, later adapted for data valuation

by Chen et al. [2020b]. However, their approach computes pointwise mutual information through a complex integral involving the product of two posteriors divided by the prior (see Appendix C for details). Schoenebeck and Yu [2020a] also estimate mutual information but is restricted to discrete variables or specific continuous distributions.

Mutual information estimation. Mutual information (MI) is a key concept in data science that measures the statistical dependence between random variables. However, estimating MI in high-dimensional settings is notoriously difficult. Non-parametric methods, such as binning, likelihood-ratio estimators with support vector machines, and kernel-density estimators, are commonly used [Fraser and Swinney, 1986, Darbellay and Vajda, 1999, Kraskov et al., 2004] for estimating mutual information, but these approaches often do not scale well with sample size and data dimensionality [Gao et al., 2015]. Variational neural estimators, such as MINE [Belghazi et al., 2018b] and InfoNCE [Oord et al., 2018], have become popular alternatives. These neural MI estimators fall into two main categories: *discriminative* and *generative* approaches [Song and Ermon, 2019]. Discriminative approaches (e.g., [Belghazi et al., 2018b, Oord et al., 2018, Liao et al., 2020]) estimate MI by approximating the density ratio directly from samples. However, these methods suffer from the *high-discrepancy issue*, where the variance of the estimator can grow exponentially in high-dimensional settings [McAllester and Stratos, 2020, Song and Ermon, 2019]. Generative approaches (e.g., [Butakov et al., 2024, Franzese et al., 2023]) aim to estimate the distributions from samples using generative models. The accuracy of these estimates heavily depends on the quality of the learned generative models, and generative modeling is well-known hard in high-dimensional cases [Chen et al., 2020a, Lipman et al., 2022]. Prior work has primarily focused on pairs of individual data points, typically in the range of thousands of dimensions (e.g., correlated image pairs from MNIST or CIFAR-10). Recent work by Gowri et al. [2024] shows that while standard MI estimators perform well in up to tens of intrinsic dimensions, they are not reliable when intrinsic dimensionality gets higher and available data is limited. To mitigate this, they suggest reducing dimensionality with pre-trained models before MI estimation, which improves scalability.

3 Model

Consider a machine learning task with a model parameterized by $\boldsymbol{\theta} \in \Theta \subseteq \mathbb{R}^k$. We assume the Bayesian framework, where a parameter $\boldsymbol{\theta}$ is drawn from an underlying prior distribution $p(\boldsymbol{\theta})$. Suppose we have a test dataset $T = (\mathbf{x}_T^{(1)}, \dots, \mathbf{x}_T^{(N_T)})$, consisting of N_T independent and identically distributed (i.i.d.) data points drawn from an underlying distribution $p(\mathbf{x}_T|\boldsymbol{\theta})$, and an original dataset $D = (\mathbf{x}_D^{(1)}, \dots, \mathbf{x}_D^{(N_D)})$, with N_D i.i.d. data points from an underlying $p(\mathbf{x}_D|\boldsymbol{\theta})$. The two datasets may not follow the same distribution, so $p(\mathbf{x}_D|\boldsymbol{\theta})$ need not equal $p(\mathbf{x}_T|\boldsymbol{\theta})$. Denote the support of D and T by \mathcal{D} and \mathcal{T} , respectively.

We aim to evaluate different data curation methods, which can be seen as functions

applied to the original dataset, possibly incorporating additional information to improve data quality. This additional information is represented by a random variable A , which may be correlated with both the model parameter θ and the dataset D . We formalize this concept below.

Definition 3.1 (Data curation method). Let A be a random variable representing additional information for data curation, and let \mathcal{A} be the support of A . A data curation method with additional information A is a function $f : \mathcal{A} \times \mathcal{D} \rightarrow \mathcal{D}$ that outputs a modified dataset $f(A, D)$ given A and an original dataset $D \in \mathcal{D}$. The space of such functions is denoted by \mathcal{F} .

Below are several examples of data curation methods:

- **Adding new data.** A simple data curation method is adding new data, where $A \in \mathcal{A} = \mathcal{D}$ represents the new data and $f(A, D) = D \cup A$.
- **Deleting data.** It is also common to select a subset of data and remove the others, as seen in coresets selection [Mirzasoleiman et al., 2020], data filtering with quality signals [Gunasekar et al., 2023, Li et al., 2023, Fang et al., 2023, Pouget et al., 2024], data deduplication [Kandpal et al., 2022], and removing low-quality or out-of-domain data [Northcutt et al., 2021, Ghorbani and Zou, 2019, Jia et al., 2019b]. In data deletion, the additional information can be represented as a random vector $A \in \{0, 1\}^{N_D}$ indicating whether each data point is retained or removed.
- **Reweighting data.** Another commonly used method is resampling data points with different weights [Xie et al., 2024, Xu et al., 2024]. Here the additional information can be represented by a random vector $A \in \mathbb{N}^{N_D}$ indicating the number of copies of each data point in the final dataset.

To rigorously distinguish between methods that merely adapt the dataset to be more similar to the test data and those that introduce meaningful improvements, we employ the *Blackwell ordering of informativeness*. Rather than relying on empirical test accuracy—which can be confounded by biases in a specific test set T —we evaluate data curation methods by their effect on the *informativeness* of the dataset D about the true underlying model parameters θ .

Definition 3.2 (Blackwell order of informativeness [Blackwell et al., 1951]). If random variables $X \rightarrow Y \rightarrow Z$ form a Markov chain, then Z is *less informative* than Y about X .

The introduction of Blackwell ordering is justified by the following theorem. Consider a method $f(A, D)$ that reduces the informativeness of D about the true model parameter θ according to the Blackwell order. Then, by Blackwell’s theorem, the optimal model trained on D can achieve an expected loss (over the true underlying distribution) that is no greater than that achievable by the optimal model trained on $f(A, D)$.

Theorem 3.3 (Informal, [Blackwell et al., 1951]). *Suppose $\theta \rightarrow D \rightarrow f(A, D)$ forms a Markov chain. Consider the decision problem of selecting a model h from a model class \mathcal{H} to minimize the expected loss using a dataset. Then, the minimum expected loss achievable using D is at least as low as that achievable using $f(A, D)$, where the expected loss is defined over the true underlying distribution by any training loss function. The formal version can be found in Appendix A.*

We therefore define *strategic data curation methods* as those that reduce the dataset's informativeness about the true model parameter θ , even if they may improve test scores.

Definition 3.4 (Strategic data curation). A data curation method $f(\cdot)$ is strategic if the curated dataset $f(A, D)$ is less informative about θ than the original dataset D . Formally, $\theta \rightarrow D \rightarrow f(A, D)$ forms a Markov chain.

Below are several examples of strategic curation methods:

- **Adding recursively generated synthetic data.** When $f(A, D)$ adds new data A to D , if A consists of synthetic data produced by a model $\hat{\theta}$ trained on D , then $f(A, D)$ is strategic because $\theta \rightarrow D \rightarrow \hat{\theta} \rightarrow A$ forms a Markov chain. As highlighted by Shumailov et al. [2024], the use of such recursively-generated data may cause *model collapse*. In contrast, if A contains synthetic data generated from unseen sources or filtered by verifiers, it may introduce new information, making $f(A, D)$ non-strategic.
- **Deleting or reweighting data without additional signals.** When deleting or reweighting data, if $A \in \mathbb{N}^{N_D}$ is guided by some additional quality or relevance signal, the filtered/reweighted dataset can be more informative, making $f(A, D)$ non-strategic. Conversely, if A is decided solely from the observed dataset D without utilizing new signals, the resulting dataset $f(A, D)$ will be less informative. Because $\theta \rightarrow D \rightarrow A$ forms a Markov chain, and thus $\theta \rightarrow D \rightarrow f(A, D)$ forms a Markov chain, making $f(A, D)$ strategic.
- **Deleting or reweighting data by non-essential features.** In addition, when deleting or reweighting data, if $A \in \mathbb{N}^{N_D}$ (the number of copies of each data point in the final dataset) is based on some non-essential feature that is non-predictive of the label, the resulting dataset will be less informative, making $f(A, D)$ strategic. To be more specific, suppose a data point $\mathbf{x} = (\mathbf{z}, y)$ in D consists of a label y and essential features \mathbf{z} . Suppose there is some non-essential feature z_N that satisfies $p(y|\theta, \mathbf{z}, z_N) = p(y|\theta, \mathbf{z})$ and is non-predictive of y conditioned on \mathbf{z} , as illustrated in the graphical model in Figure 1. Then if the vector $A \in \mathbb{N}^{N_D}$ is decided by this non-essential feature of the data points, $z_N^{(1)}, \dots, z_N^{(N_D)}$ (as well as D), then the resulting dataset will be less informative because $z_N^{(1)}, \dots, z_N^{(N_D)}$ are independent of θ conditioned on D (as the path between θ and z_N is blocked by \mathbf{z} and d-separation implies conditional independence).

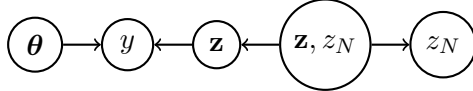


Figure 1: Graphical model for non-essential features.

The remaining question is how to determine whether θ , D , and $f(A, D)$ form a Markov chain. Rather than addressing this relation directly, we consider designing a *scoring function* that quantifies the informativeness of curated datasets. Specifically, we evaluate data curation methods by assigning a score that reflects their impact on informativeness, with the goal of distinguishing between methods that increase or reduce informativeness.

Definition 3.5 (Scoring function for data curation methods). A scoring function for data curation methods $S : \mathcal{F} \times \Delta(\mathcal{D} \times \mathcal{T}) \rightarrow \mathbb{R}$ assigns a score $S(f(\cdot), D, T)$ to a data curation method $f(\cdot)$,² given access to the original data D and test data T . For simplicity, we omit D and T and write $S(f(\cdot))$ when clear from the context.

In this work, we aim to design a scoring function that does not encourage strategic data curation methods. Specifically, we seek a function that assigns lower scores to strategic methods than to the case of no modification.

Definition 3.6 (Strategy-proof scoring functions). A scoring function $S(f(\cdot))$ is *strategy-proof* if:

- For any strategic method $f(\cdot)$, we have $S(f(\cdot)) \leq S(\text{id}(\cdot))$, where $\text{id}(A, D) \equiv D$;
- $S(\cdot)$ is non-constant (i.e., not all methods receive the same score).

Given D , T , and a data curation method $f(\cdot)$, a natural scoring function is to train a model on curated data $f(A, D)$ and use its test accuracy on T as the score. However, as we demonstrate in Section 5.2, this approach is not strategy-proof: it may incentivize curation strategies that make D more similar to T , improving test accuracy while reducing the informativeness of the dataset.

4 PMI Dataset Score

Designing a strategy-proof scoring function is not straightforward. We propose using the *Shannon mutual information* (MI) of the curated data $f(D)$ and the test data T , which can be proved to constitute a strategy-proof scoring function. However, estimating MI in high-dimensional settings is challenging. To overcome this challenge, we introduce a novel

²The notation $\Delta(\mathcal{D} \times \mathcal{T})$ represents the space of all distributions over $\mathcal{D} \times \mathcal{T}$. This means that we allow the scoring function to sample datasets from the underlying distribution and determine the score via the samples.

method for approximating the *pointwise mutual information* of datasets, enabling accurate and efficient estimation built on established Bayesian machine learning methods. In this section, we omit A and use $f(D)$ to represent a data curation method for simplicity.

4.1 Mutual information as the metric

We first propose using the *Shannon mutual information* of the curated dataset $\widehat{D} = f(D)$ and the observable test dataset T as our scoring function, which serves as a strategy-proof scoring function.³

Proposition 4.1. *Given a data curation method $f(\cdot)$, let $\widehat{D} = f(D)$. Then the Shannon mutual information $I(\widehat{D}, T)$, when computable, constitutes a strategy-proof scoring function. Formally,*

$$I(\widehat{D}; T) = \mathbb{E}_{\widehat{D}, T} [PMI(\widehat{D}, T)] := \mathbb{E}_{\widehat{D}, T} \left[\log \frac{p(\widehat{D}, T)}{p(\widehat{D})p(T)} \right]$$

where:

- $PMI(\widehat{D}, T) = \log \frac{p(\widehat{D}, T)}{p(\widehat{D})p(T)}$ denotes the *pointwise mutual information*.
- The expectation is taken over the joint distribution $p(\widehat{D}, T)$ induced by $f(\cdot)$ and the data generating process in Section 3, with $T = (\mathbf{x}_T^{(1)}, \dots, \mathbf{x}_T^{(N_T)})$ and $D = (\mathbf{x}_D^{(1)}, \dots, \mathbf{x}_D^{(N_D)})$ being datasets of multiple data points.

The proof is deferred to Appendix D.1.

Main challenge: high-dimensional MI estimation is difficult. Then the problem boils down to estimating the mutual information of two datasets \widehat{D}, T that contain **many data points**, where the total dimensionality scales as $\dim(T) = \dim(\mathbf{x}_T) \cdot N_T$, with N_T being the number of data points and $\dim(\mathbf{x}_T)$ the dimensionality of each individual data point. However, estimating MI in high-dimensional settings is notoriously difficult. Each existing method has significant limitations. These methods aim to estimate $I(Y, Z)$ given k samples $(Y_1, Z_1), \dots, (Y_k, Z_k) \sim p(Y, Z)$.

- Discriminative approaches (e.g., [Belghazi et al., 2018b, Oord et al., 2018, Liao et al., 2020]) estimate $I(Y, Z)$ by approximating the density ratio $\frac{p(y, z)}{p(y)p(z)}$ directly from samples. However, these methods suffer from the *high-discrepancy issue*, where the variance of the estimator can grow exponentially in high-dimensional settings [McAllester and Stratos, 2020, Song and Ermon, 2019].

³Another metric that might yield a strategy-proof scoring function is the Shannon mutual information between the model parameters $\boldsymbol{\theta}$ and the curated dataset $f(D)$, denoted $I(\boldsymbol{\theta}, f(D))$. However, this metric does not prevent strategic data curation methods unless the underlying true model parameter $\boldsymbol{\theta}$ is observable. We defer the detailed discussion to Appendix B.

- Generative approaches (e.g., [Butakov et al., 2024, Franzese et al., 2023]) aim to estimate $p(y, z)$, $p(y)$, and $p(z)$ from samples using generative models. The accuracy of these estimates heavily depends on the quality of the learned generative models, and generative modeling as done by e.g. flow-based model is well-known hard in high-dimensional cases [Chen et al., 2020a, Lipman et al., 2022].

Prior work has primarily focused on pairs of individual data points with dimensionality on the order of thousands (e.g., correlated image pairs from MNIST or CIFAR-10)—a challenging task in itself. Our setting presents a more severe challenge: the aggregate dimensionality of the full datasets becomes prohibitively large due to the number of data points.

4.2 Closed-form approximation of pointwise mutual information

To overcome this challenge, we propose a novel mutual information estimation method that leverages a dataset’s ability to train a machine learning model. A key contribution is a novel closed-form expression for pointwise mutual information (PMI), enabling accurate and efficient estimation built on established Bayesian machine learning methods [Jospin et al., 2022].

Our method begins by generating k dataset pairs $(D_1, T_1), \dots, (D_k, T_k)$ and estimating mutual information $I(f(D), T)$ via the average: $\frac{1}{k} \sum_{i=1}^k \text{PMI}(f(D_i), T_i)$ defined in Proposition 4.1. To approximate PMI, we embed the data using pretrained models and then train Bayesian models (such as Bayesian logistic regression outlined in Appendix D.4 and Bayesian neural networks) on these embeddings. Let the Bayesian model have parameters $\mathbf{w} \in \mathcal{W}$, prior $p(\mathbf{w})$, and likelihoods $p(\mathbf{x}_D|\mathbf{w})$ and $p(\mathbf{x}_T|\mathbf{w})$ for the embedded data.

Finally, we compute PMI by a novel closed-form formula, assuming that $p(\mathbf{w}|\cdot)$ can be approximated by tractable distributions via established posterior inference techniques for Bayesian models.⁴

Theorem 4.2 (PMI dataset score). *Let $f(\cdot)$ be a data curation method producing curated datasets $\widehat{D}_i = f(D_i)$. Suppose we have a Bayesian model over the embedded data with parameters $\mathbf{w} \in \mathcal{W}$, prior $p(\mathbf{w})$, and likelihoods $p(\mathbf{x}_D|\mathbf{w})$ and $p(\mathbf{x}_T|\mathbf{w})$. Let $p(\mathbf{w}|X)$ denote the posterior distribution of \mathbf{w} given embedded dataset X . Then $\text{PMI}(\widehat{D}_i, T_i)$ can be*

⁴Extensive research in Bayesian machine learning has focused on estimating the posterior distribution of model parameters $p(\mathbf{w}|\cdot)$. For instance, Laplace approximation and variational inference approximate the posterior $p(\mathbf{w}|\cdot)$ by tractable distributions. But even with a tractable approximate posterior $p(\mathbf{w}|\cdot)$, the posterior predictive $p(T_i|f(D_i)) = \int_{\theta} p(T_i|\mathbf{w})p(\mathbf{w}|f(D_i)) d\mathbf{w}$ in PMI remains intractable for most models, including logistic regression. Common approximation approaches each have limitations in our setting: (1) Monte Carlo integration suffers from numerical instability with near-zero likelihoods $p(T_i|\mathbf{w})$; probit approximation and Laplace bridge methods are limited to single-point predictions $\int_{\mathbf{w}} p(x_T^{(i)}|\mathbf{w})p(\mathbf{w}|D) d\mathbf{w}$ whereas we require joint predictions $\int_{\mathbf{w}} \prod_i p(x_T^{(i)}|\mathbf{w})p(\mathbf{w}|D) d\mathbf{w}$, for entire datasets.

computed as

$$PMI(\widehat{D}_i, T_i) = U_\eta(\widehat{D}_i, T_i) := \log \frac{p(\mathbf{w} = \eta | \widehat{D}_i) \cdot p(\mathbf{w} = \eta | T_i)}{p(\mathbf{w} = \eta) \cdot p(\mathbf{w} = \eta | \widehat{D}_i, T_i)}, \quad (1)$$

where η is an arbitrary parameter value in \mathcal{W} .⁵ For simplicity, here we use \widehat{D}_i and T_i to denote the embedded datasets.

The proof of Theorem 4.2 only relies on Bayes’ rule and we defer the proof to Appendix D.2.

Our PMI dataset score can be easily computed as long as the posteriors and the prior are approximated by tractable distributions. This makes it applicable to a wide range of commonly-used Bayesian neural networks, including those employing Gaussian approximations [Daxberger et al., 2021, Yang et al., 2023, Blundell et al., 2015, Wang et al., 2024f], Gaussian mixture approximations [Blundell et al., 2015], and Dirichlet approximations [Hobbhahn et al., 2022].

4.3 Algorithm and convergence rate

Combining all the steps, our PMI scoring function for data curation methods can be computed as in Algorithm 1. When the Bayesian model provides accurate posterior

Algorithm 1 PMI scoring function

Require: Datasets $(D_1, T_1), \dots, (D_k, T_k)$, a data curation method $f(\cdot)$ for evaluation, a pre-trained model to generate embeddings of data, a Bayesian model over the embeddings parameterized by $\mathbf{w} \in \mathcal{W}$ with tractable posterior approximations $p(\mathbf{w} | \cdot)$, a value $\eta \in \mathcal{W}$.

Ensure: A score for the curation method $f(\cdot)$

- 1: Apply the curation method $f(\cdot)$ on D_1, \dots, D_k and get the curated datasets $\widehat{D}_1, \dots, \widehat{D}_k$
- 2: Use the pre-trained model to embed the datasets $\widehat{D}_1, \dots, \widehat{D}_k$ and T_1, \dots, T_k .
- 3: For each pair of embedded (\widehat{D}_i, T_i) , train separate Bayesian models on \widehat{D}_i , T_i , and their union $\widehat{D}_i \cup T_i$ to get the posterior probabilities $p(\mathbf{w} = \eta | \widehat{D}_i)$, $p(\mathbf{w} = \eta | T_i)$, and $p(\mathbf{w} = \eta | \widehat{D}_i, T_i)$. Compute the pointwise mutual information $U_\eta(\widehat{D}_i, T_i)$ using Equation (1).
- 4: Return $\frac{1}{k} \sum_{i=1}^k U_\eta(\widehat{D}_i, T_i)$.

probabilities $p(\mathbf{w} = \eta | \widehat{D}_i)$, $p(\mathbf{w} = \eta | T_i)$, and $p(\mathbf{w} = \eta | \widehat{D}_i, T_i)$, the algorithm outputs an unbiased estimator of the target metric $I(f(D), T)$, which converges to the true value of $I(f(D), T)$ as k increases.

⁵Our expression in Theorem 4.2 also allows new interpretations of PMI, which we defer to Appendix E.1.

Corollary 4.3. *Assume that the Bayesian model provides accurate posterior probabilities. Then the output of Algorithm 1 provides an unbiased estimator of $I(f(D), T)$. Moreover, assuming that the posteriors are in an exponential family and the datasets have bounded sufficient statistics,⁶ we have $\Pr\left(\left|\frac{1}{k} \sum_{i=1}^k U_\eta(\hat{D}_i, T_i) - I(\hat{D}, T)\right| \leq \varepsilon\right) \geq 1 - \delta$ when $k = O(\log(1/\delta)/\varepsilon^2)$, and we have the expected square error of the estimator decreases as $O(1/k)$.*

The proof is deferred to Appendix D.3. Compared to commonly used MI estimators, our concentration bound is independent of the variable dimensionality, unlike the bound in Belghazi et al. [2018a], which scales as $O\left(\frac{d \log(\sqrt{d}/\varepsilon) + d + \log(1/\delta)}{\varepsilon^2}\right)$, where d is the variable dimensionality.⁷ We demonstrate the advantages of our method in Section 5.1

5 Experiments

We evaluate the accuracy of our MI estimator and its ability to assess dataset informativeness through experiments on two image classification datasets, MNIST and CIFAR-10. Our results demonstrate that the proposed PMI dataset score remains effective even when employing the simple Bayesian logistic regression model (outlined in Appendix D.4) on embedded data generated by pretrained models such as ResNet. The posterior approximation can be efficiently computed by training a standard logistic regression model with L2 regularization or by employing the Laplace approximation method in [Daxberger et al., 2021].

5.1 Accuracy of Mutual Information Estimation

We first evaluate the accuracy of our dataset MI estimator on resampled real-world data.

A benchmark for dataset MI estimation. Prior work on MI estimation has primarily focused on pairs of individual data points with dimensionality on the order of 1000 (e.g., correlated image pairs from MNIST or CIFAR-10). However, these methods have never been evaluated in settings where the goal is to estimate the mutual information between datasets containing many such data points. To bridge this gap, we introduce a benchmark that extends existing MI evaluation frameworks [Lee and Rhee, 2024, Gowri et al., 2024] to dataset pairs. Our benchmark generates dataset pairs with pre-defined MI values by resampling from standard datasets like MNIST and CIFAR. We construct datasets with binary labels (e.g., label 0 and 1) as follows. Given a target MI value λ , we first define a joint

⁶The assumption of bounded sufficient statistics is similar to that in Belghazi et al. [2018b], who assume that the output of the *statistics network* is bounded (see the assumptions in their Theorem 3). When the sufficient statistics are not bounded, we can still obtain a result of the same order by clipping $U_\eta(\cdot)$. See details in Appendix D.3.

⁷The dependence on d mainly comes from a uniform convergence bound that requires covering a subspace of \mathbb{R}^d with a finite number of small balls. See their proof of Theorem 6.

distribution $p(r_D, r_T)$ of two correlated numbers $r_D, r_T \in \{0.1, 0.2, \dots, 0.9\}$ such that their mutual information $I(r_D, r_T) = \lambda$. Here, r_D and r_T represent the proportions of 0-labeled images in datasets D and T , respectively. Next, we sample $r_D, r_T \sim p(r_D, r_T)$ and sample images to enforce the conditional entropy $H(r_D|D) = 0$ and $H(r_T|T) = 0$. This ensures that the ground-truth mutual information $I(D, T) = I(r_D, r_T)$. We generate $k = 2000$ datasets pairs with sizes ranging from 50 to 100 and ground-truth mutual information $I(D, T) \in [0, 1]$, and assess estimation accuracy by the rank correlation between the estimated and true MI rankings. See Appendix F.1 for details.

Baseline method. Due to the high dimensionality of datasets, we apply dimensionality reduction techniques before evaluation. For CMNIST, we use Principal Component Analysis to reduce the feature dimensionality to 100. For CIFAR, we extract embeddings by a ResNet-18 model pretrained on ImageNet, with the final classification layer removed. We then consider the following baselines.

- **MINE:** For unstructured high-dimensional data such as images, MINE [Belghazi et al., 2018b] is one of the most widely-used and effective MI estimators [Gowri et al., 2024, Lee and Rhee, 2024]. According to Lee and Rhee [2024], MINE is also the most robust method for image-based data, making it a strong baseline for our setting.
- **MINE on trained model parameters w :** To further reduce dimensionality, we apply MINE not on raw data but on the trained model parameters, which serve as a lower-dimensional proxy.
- **LMI:** To further reduce dimensionality, we adopt a recent approach by Gowri et al. [2024], which learns low-dimensional latent representations of the data before estimating mutual information.
- **Monte Carlo integration:** We also evaluate a simple Monte Carlo integration approach to compute the pointwise mutual information defined in Proposition 4.1. See details in Appendix F.1.

Our method. We implement our PMI estimator following Algorithm 1. To obtain the posterior distributions $p(\mathbf{w}|\cdot)$, we train logistic regression models on embedded D and T with L2 regularization parameterized by C . This setup corresponds to Bayesian logistic regression with Gaussian approximation, where the prior is $N(0, C \cdot \mathbf{I})$. See Appendix D.4.

Results. As shown in Table 1 and Figure 2, our PMI estimator achieves the highest Spearman’s ρ rank correlation, producing the most accurate estimates with the smallest variance. In addition, in Appendix F.1, we show that PMI outperforms other methods regardless of the choice of regularization strength C , which means its ranking estimates are robust to prior misspecification. Our method also remains effective across different dataset sizes.

	CMNIST	CIFAR
PMI	0.967 \pm 0.015	0.976 \pm 0.000
MINE	0.354 \pm 0.022	0.281 \pm 0.040
MINE on \mathbf{w}	0.367 \pm 0.033	0.312 \pm 0.043
LMI	0.765 \pm 0.174	0.634 \pm 0.033
Monte Carlo	0.611 \pm 0.029	Failed

Table 1: Spearman’s rank correlation (ρ) between estimated and ground-truth mutual information rankings for different estimation methods on Colored MNIST [Arjovsky et al., 2020] and CIFAR [Krizhevsky, 2009]. Higher values indicate better alignment with the true MI ranking. PMI achieves the strongest correlation. We run 20 independent trials to compute the standard deviation, which quantifies the variability of estimation outcomes across repeated measurements. The Monte Carlo method fails on CIFAR, consistently outputting zero due to numerical instability caused by near-zero likelihoods. The dataset size is 100.

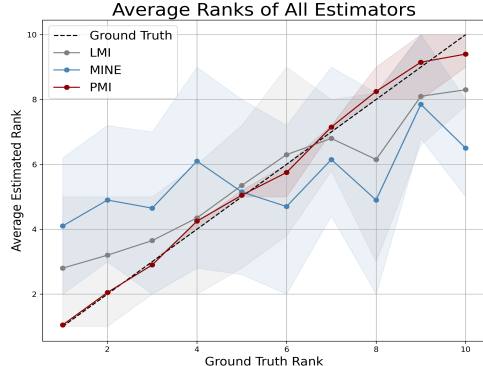


Figure 2: Estimated rankings from different methods on CIFAR. PMI produces the most accurate estimates with the smallest variance. The x -axis denotes the ground-truth MI ranking indices, and the y -axis denotes the estimated rankings generated by each method. The lines represent the average estimated rankings over 20 trials, while the shaded regions indicate the range of their estimations. The dataset size is 100. See the results for Colored MNIST in Appendix F.1.

5.2 Evaluating data curation methods

We next test our PMI scoring function in evaluating data curation methods. We show that the PMI scoring function is effective in distinguishing between strategic and non-strategic curation methods, whereas evaluating curation methods using test scores could promote strategic methods that do not add new information but merely make the data more similar to the test data.

Data curation methods and dataset generation. There are numerous data curation methods available for evaluation. We select three that can be clearly categorized as strategic or non-strategic, allowing us to verify whether they are correctly classified. To run our PMI-based and test-score-based evaluations, we sample dataset pairs from Colored MNIST [Arjovsky et al., 2020] and Corrupted CIFAR [Hendrycks and Dietterich, 2019].

- **Data filtering:** We consider the removal of mislabeled data, a non-strategic curation method that is expected to yield a higher score than leaving the data unmodified. We randomly sample T_1, \dots, T_k from the test set, and sample datasets from the training

set and flip the labels of some data points to generate D_1, \dots, D_k . We compare the scores before and after the removal of these mislabeled data points.

- **Strategic data duplication or removal by non-essential features:** We next consider a strategic curation method that duplicates or removes data based solely on non-essential features—such as image brightness in Corrupted CIFAR or color in Colored MNIST—to make the training data resemble the test data. This method, which does not use quality or relevance signals, is expected to score lower than $f(D) \equiv D$. Let \mathbf{z}_E denote essential features, $z_N \in \{0, 1\}$ a binary non-essential feature, and $y \in \{0, 1\}$ the label. We sample dataset pairs (D, T) such that $p_D(\mathbf{z}_E, y) = p_T(\mathbf{z}_E, y)$, but $p_D(z_N|\mathbf{z}_E, y) \neq p_T(z_N|\mathbf{z}_E, y)$. We then adjust D via duplication/removal to align $p_D(z_N|\mathbf{z}_E, y)$ with $p_T(z_N|\mathbf{z}_E, y)$. Conditioned on D , such duplication/removal is independent of the true θ , making it a strategic curation method.

For both cases, we generate the smallest datasets that achieve reasonable accuracy $\sim 80\% - 90\%$ to avoid overlap.

Scoring functions. We compare our PMI dataset score with the test-score-based evaluation defined as: $S_{TS}(f(\cdot)) = \frac{1}{k} \sum_{i=1}^k \text{Acc}(\hat{\theta}(f(D_i)), T_i)$, where $\text{Acc}(\hat{\theta}(D), T)$ denotes the accuracy of a model trained on D and evaluated on T . To compute the PMI score, we train a logistic regression for Colored MNIST, and a logistic regression on ResNet18 embeddings for Corrupted CIFAR. As in Section 5.1, all logistic regression models are trained with L2 regularization parameter C , corresponding to a Gaussian prior $N(0, C \cdot \mathbf{I})$. These models are also used to compute test accuracy.

Results. Table 2 reports changes in the PMI score and test accuracy S_{TS} after applying three data curation methods. The PMI score effectively distinguishes between strategic and non-strategic data curation methods: data filtering increases the score, while duplication or removal based on non-essential features decreases it. In contrast, test accuracy fails to detect strategic data curation methods, consistently assigning higher scores. This highlights the risk of relying solely on test accuracy, which may inadvertently promote strategic methods that do not introduce new information but merely make the training data more similar to the test data. Our results are robust to prior misspecification (i.e., different choices of regularization parameter) and generalize across data distributions, as detailed in Appendix F.2.

6 Discussion and Future Work

We propose an information-theoretic framework for evaluating data curation methods that measures data informativeness by the mutual information of the curated data and the test data. We discuss several potential directions for future work. Firstly, a key open problem

Dataset	Operation	Δ PMI Score	Δ Test Accuracy (%)
Colored MNIST	Denoising	13.59 \pm 1.04	0.31 \pm 0.02
	Duplication	-2.59 \pm 1.14	1.43 \pm 0.29
	Removal	-13.96 \pm 2.05	0.54 \pm 0.04
Corrupted CIFAR	Denoising	1.53 \pm 0.15	7.29 \pm 0.10
	Duplication	-0.90 \pm 0.04	0.58 \pm 0.03
	Removal	-4.68 \pm 0.12	0.82 \pm 0.13
Strategy-proof		Yes	No

Table 2: Change in PMI score and test accuracy S_{TS} after applying three data curation methods to Colored MNIST and Corrupted CIFAR datasets. The PMI score effectively distinguishes between **strategic** and **non-strategic** methods: data filtering increases the PMI score, while duplication or removal based on non-essential features decreases it. In contrast, test accuracy fails to detect **strategic** methods, always assigning higher scores. Results are averaged over $k = 1,000$ samples. Details of the experimental setup are provided in Appendix F.2.

is to develop principled method for selecting dataset pairs that most effectively estimate mutual information. We have observed that the PMI scoring function can fail when the datasets D_i, T_i are too small to train effective models, as well as when they are too large, resulting in significant overlap between datasets that violates the independence assumption. Secondly, the selection of the prior is also crucial. While we observe that the PMI scoring function is robust to prior misspecifications in terms of ranking mutual information, the absolute accuracy of its MI estimates is highly sensitive to the choice of prior. Thirdly, our experiments focus on the simple logistic regression for Bayesian modeling. It remains an open question whether mutual information estimation could be improved by more advanced Bayesian neural networks.

References

Alon Albalak, Yanai Elazar, Sang Michael Xie, Shayne Longpre, Nathan Lambert, Xinyi Wang, Niklas Muennighoff, Bairu Hou, Liangming Pan, Haewon Jeong, et al. A survey on data selection for language models. *arXiv preprint arXiv:2402.16827*, 2024.

Martin Arjovsky, Léon Bottou, Ishaan Gulrajani, and David Lopez-Paz. Invariant risk minimization, 2020. URL <https://arxiv.org/abs/1907.02893>.

Mohamed Ishmael Belghazi, Aristide Baratin, Sai Rajeshwar, Sherjil Ozair, Yoshua Bengio, Aaron Courville, and Devon Hjelm. Mutual information neural estimation. In *International conference on machine learning*, pages 531–540. PMLR, 2018a.

Mohamed Ishmael Belghazi, Aristide Baratin, Sai Rajeswar, Sherjil Ozair, Yoshua Bengio, Aaron Courville, and R Devon Hjelm. Mine: mutual information neural estimation. *arXiv preprint arXiv:1801.04062*, 2018b.

David Blackwell et al. Comparison of experiments. In *Proceedings of the second Berkeley symposium on mathematical statistics and probability*, volume 1, page 26, 1951.

Charles Blundell, Julien Cornebise, Koray Kavukcuoglu, and Daan Wierstra. Weight uncertainty in neural network. In *International conference on machine learning*, pages 1613–1622. PMLR, 2015.

Tom Brown, Benjamin Mann, Nick Ryder, Melanie Subbiah, Jared D Kaplan, Prafulla Dhariwal, Arvind Neelakantan, Pranav Shyam, Girish Sastry, Amanda Askell, et al. Language models are few-shot learners. *Advances in neural information processing systems*, 33:1877–1901, 2020.

Ivan Butakov, Aleksandr Tolmachev, Sofia Malanchuk, Anna Neopryatnaya, and Alexey Frolov. Mutual information estimation via normalizing flows. *Advances in Neural Information Processing Systems*, 37:3027–3057, 2024.

Yanzhi Chen, Dinghuai Zhang, Michael Gutmann, Aaron Courville, and Zhanxing Zhu. Neural approximate sufficient statistics for implicit models. *arXiv preprint arXiv:2010.10079*, 2020a.

Yiling Chen, Yiheng Shen, and Shuran Zheng. Truthful data acquisition via peer prediction. *Advances in Neural Information Processing Systems*, 33:18194–18204, 2020b.

Georges A Darbellay and Igor Vajda. Estimation of the information by an adaptive partitioning of the observation space. *IEEE Transactions on Information Theory*, 45(4):1315–1321, 1999.

Erik Daxberger, Agustinus Kristiadi, Alexander Immer, Runa Eschenhagen, Matthias Bauer, and Philipp Hennig. Laplace redux-effortless bayesian deep learning. *Advances in Neural Information Processing Systems*, 34:20089–20103, 2021.

Alex Fang, Albin Madappally Jose, Amit Jain, Ludwig Schmidt, Alexander Toshev, and Vaishaal Shankar. Data filtering networks. *arXiv preprint arXiv:2309.17425*, 2023.

Vitaly Feldman and Chiyuan Zhang. What neural networks memorize and why: Discovering the long tail via influence estimation. *Advances in Neural Information Processing Systems*, 33:2881–2891, 2020.

Giulio Franzese, Mustapha Bounoua, and Pietro Michiardi. Minde: Mutual information neural diffusion estimation. *arXiv preprint arXiv:2310.09031*, 2023.

Andrew M Fraser and Harry L Swinney. Independent coordinates for strange attractors from mutual information. *Physical review A*, 33(2):1134, 1986.

Shuyang Gao, Greg Ver Steeg, and Aram Galstyan. Efficient estimation of mutual information for strongly dependent variables. In *Artificial intelligence and statistics*, pages 277–286. PMLR, 2015.

Tianyu Gao, Alexander Wettig, Luxi He, Yihe Dong, Sadhika Malladi, and Danqi Chen. Metadata conditioning accelerates language model pre-training. *CoRR*, abs/2501.01956, 2025. doi: 10.48550/ARXIV.2501.01956. URL <https://doi.org/10.48550/arXiv.2501.01956>.

Felipe Garrido-Lucero, Benjamin Heymann, Maxime Vono, Patrick Loiseau, and Vianney Perchet. Du-shapley: A shapley value proxy for efficient dataset valuation, 2024. URL <https://arxiv.org/abs/2306.02071>.

Amirata Ghorbani and James Zou. Data shapley: Equitable valuation of data for machine learning. In *International conference on machine learning*, pages 2242–2251. PMLR, 2019.

Gokul Gowri, Xiaokang Lun, Allon Klein, and Peng Yin. Approximating mutual information of high-dimensional variables using learned representations. *Advances in Neural Information Processing Systems*, 37:132843–132875, 2024.

Aaron Grattafiori, Abhimanyu Dubey, Abhinav Jauhri, Abhinav Pandey, Abhishek Kadian, Ahmad Al-Dahle, Aiesha Letman, Akhil Mathur, Alan Schelten, Alex Vaughan, Amy Yang, Angela Fan, Anirudh Goyal, Anthony Hartshorn, Aobo Yang, Archi Mitra, Archie Sravankumar, Artem Korenev, Arthur Hinsvark, Arun Rao, Aston Zhang, Aurelien Rodriguez, Austen Gregerson, Ava Spataru, Baptiste Roziere, Bethany Biron, Binh Tang, Bobbie Chern, Charlotte Caucheteux, Chaya Nayak, Chloe Bi, Chris Marra,

Chris McConnell, Christian Keller, Christophe Touret, Chunyang Wu, Corinne Wong, Cristian Canton Ferrer, Cyrus Nikolaidis, Damien Allonsius, Daniel Song, Danielle Pintz, Danny Livshits, Danny Wyatt, David Esiobu, Dhruv Choudhary, Dhruv Mahajan, Diego Garcia-Olano, Diego Perino, Dieuwke Hupkes, Egor Lakomkin, Ehab AlBadawy, Elina Lobanova, Emily Dinan, Eric Michael Smith, Filip Radenovic, Francisco Guzmán, Frank Zhang, Gabriel Synnaeve, Gabrielle Lee, Georgia Lewis Anderson, Govind Thattai, Graeme Nail, Gregoire Mialon, Guan Pang, Guillem Cucurell, Hailey Nguyen, Hannah Korevaar, Hu Xu, Hugo Touvron, Iliyan Zarov, Imanol Arrieta Ibarra, Isabel Kloumann, Ishan Misra, Ivan Evtimov, Jack Zhang, Jade Copet, Jaewon Lee, Jan Geffert, Jana Vranes, Jason Park, Jay Mahadeokar, Jeet Shah, Jelmer van der Linde, Jennifer Billock, Jenny Hong, Jenya Lee, Jeremy Fu, Jianfeng Chi, Jianyu Huang, Jiawen Liu, Jie Wang, Jiecao Yu, Joanna Bitton, Joe Spisak, Jongsoo Park, Joseph Rocca, Joshua Johnstun, Joshua Saxe, Junteng Jia, Kalyan Vasuden Alwala, Karthik Prasad, Kartikeya Upasani, Kate Plawiak, Ke Li, Kenneth Heafield, Kevin Stone, Khalid El-Arini, Krithika Iyer, Kshitiz Malik, Kuenley Chiu, Kunal Bhalla, Kushal Lakhota, Lauren Rantala-Yearly, Laurens van der Maaten, Lawrence Chen, Liang Tan, Liz Jenkins, Louis Martin, Lovish Madaan, Lubo Malo, Lukas Blecher, Lukas Landzaat, Luke de Oliveira, Madeline Muzzi, Mahesh Pasupuleti, Mannat Singh, Manohar Paluri, Marcin Kardas, Maria Tsimpoukelli, Mathew Oldham, Mathieu Rita, Maya Pavlova, Melanie Kambadur, Mike Lewis, Min Si, Mitesh Kumar Singh, Mona Hassan, Naman Goyal, Narjes Torabi, Nikolay Bashlykov, Nikolay Bogoychev, Niladri Chatterji, Ning Zhang, Olivier Duchenne, Onur Çelebi, Patrick Alrassy, Pengchuan Zhang, Pengwei Li, Petar Vasic, Peter Weng, Prajjwal Bhargava, Pratik Dubal, Praveen Krishnan, Punit Singh Koura, Puxin Xu, Qing He, Qingxiao Dong, Ragavan Srinivasan, Raj Ganapathy, Ramon Calderer, Ricardo Silveira Cabral, Robert Stojnic, Roberta Raileanu, Rohan Maheswari, Rohit Girdhar, Rohit Patel, Romain Sauvestre, Ronnie Polidoro, Roshan Sumbaly, Ross Taylor, Ruan Silva, Rui Hou, Rui Wang, Saghar Hosseini, Sahana Chennabasappa, Sanjay Singh, Sean Bell, Seohyun Sonia Kim, Sergey Edunov, Shaoliang Nie, Sharan Narang, Sharath Raparthy, Sheng Shen, Shengye Wan, Shruti Bhosale, Shun Zhang, Simon Vandenhende, Soumya Batra, Spencer Whitman, Sten Sootla, Stephane Collot, Suchin Gururangan, Sydney Borodinsky, Tamar Herman, Tara Fowler, Tarek Sheasha, Thomas Georgiou, Thomas Scialom, Tobias Speckbacher, Todor Mihaylov, Tong Xiao, Ujjwal Karn, Vedanuj Goswami, Vibhor Gupta, Vignesh Ramanathan, Viktor Kerkez, Vincent Gonguet, Virginie Do, Vish Vogeti, Vítor Albiero, Vladan Petrovic, Weiwei Chu, Wenhan Xiong, Wenyin Fu, Whitney Meers, Xavier Martinet, Xiaodong Wang, Xiaofang Wang, Xiaoqing Ellen Tan, Xide Xia, Xinfeng Xie, Xuchao Jia, Xuewei Wang, Yaelle Goldschlag, Yashesh Gaur, Yasmine Babaee, Yi Wen, Yiwen Song, Yuchen Zhang, Yue Li, Yuning Mao, Zacharie Delpierre Coudert, Zheng Yan, Zhengxing Chen, Zoe Papakipos, Aaditya Singh, Aayushi Srivastava, Abha Jain, Adam Kelsey, Adam Shajnfeld, Adithya Gangidi, Adolfo Victoria, Ahuva Goldstand, Ajay Menon, Ajay Sharma, Alex Boesenber, Alexei Baevski, Allie Feinstein, Amanda Kallet, Amit Sangani, Amos Teo, Anam Yunus, Andrei Lupu, Andres Alvarado, Andrew

Caples, Andrew Gu, Andrew Ho, Andrew Poulton, Andrew Ryan, Ankit Ramchandani, Annie Dong, Annie Franco, Anuj Goyal, Aparajita Saraf, Arkabandhu Chowdhury, Ashley Gabriel, Ashwin Bharambe, Assaf Eisenman, Azadeh Yazdan, Beau James, Ben Maurer, Benjamin Leonhardi, Bernie Huang, Beth Loyd, Beto De Paola, Bhargavi Paranjape, Bing Liu, Bo Wu, Boyu Ni, Braden Hancock, Bram Wasti, Brandon Spence, Brani Stojkovic, Brian Gamido, Britt Montalvo, Carl Parker, Carly Burton, Catalina Mejia, Ce Liu, Changhan Wang, Changkyu Kim, Chao Zhou, Chester Hu, Ching-Hsiang Chu, Chris Cai, Chris Tindal, Christoph Feichtenhofer, Cynthia Gao, Damon Civin, Dana Beaty, Daniel Kreymer, Daniel Li, David Adkins, David Xu, Davide Testuggine, Delia David, Devi Parikh, Diana Liskovich, Didem Foss, Dingkang Wang, Duc Le, Dustin Holland, Edward Dowling, Eissa Jamil, Elaine Montgomery, Eleonora Presani, Emily Hahn, Emily Wood, Eric-Tuan Le, Erik Brinkman, Esteban Arcaute, Evan Dunbar, Evan Smothers, Fei Sun, Felix Kreuk, Feng Tian, Filippos Kokkinos, Firat Ozgenel, Francesco Caggioni, Frank Kanayet, Frank Seide, Gabriela Medina Florez, Gabriella Schwarz, Gada Badeer, Georgia Swee, Gil Halpern, Grant Herman, Grigory Sizov, Guangyi, Zhang, Guna Lakshminarayanan, Hakan Inan, Hamid Shojanazeri, Han Zou, Hannah Wang, Hanwen Zha, Haroun Habeeb, Harrison Rudolph, Helen Suk, Henry Aspegren, Hunter Goldman, Hongyuan Zhan, Ibrahim Damlaj, Igor Molybog, Igor Tufanov, Ilias Leontiadis, Irina-Elena Veliche, Itai Gat, Jake Weissman, James Geboski, James Kohli, Janice Lam, Japhet Asher, Jean-Baptiste Gaya, Jeff Marcus, Jeff Tang, Jennifer Chan, Jenny Zhen, Jeremy Reizenstein, Jeremy Teboul, Jessica Zhong, Jian Jin, Jingyi Yang, Joe Cummings, Jon Carvill, Jon Shepard, Jonathan McPhie, Jonathan Torres, Josh Ginsburg, Junjie Wang, Kai Wu, Kam Hou U, Karan Saxena, Kartikay Khandelwal, Katayoun Zand, Kathy Matosich, Kaushik Veeraraghavan, Kelly Michelena, Keqian Li, Kiran Jagadeesh, Kun Huang, Kunal Chawla, Kyle Huang, Lailin Chen, Lakshya Garg, Lavender A, Leandro Silva, Lee Bell, Lei Zhang, Liangpeng Guo, Licheng Yu, Liron Moshkovich, Luca Wehrstedt, Madian Khabsa, Manav Avalani, Manish Bhatt, Martynas Mankus, Matan Hasson, Matthew Lennie, Matthias Reso, Maxim Groshev, Maxim Naumov, Maya Lathi, Meghan Keneally, Miao Liu, Michael L. Seltzer, Michal Valko, Michelle Restrepo, Mihir Patel, Mik Vyatskov, Mikayel Samvelyan, Mike Clark, Mike Macey, Mike Wang, Miquel Jubert Hermoso, Mo Metanat, Mohammad Rastegari, Munish Bansal, Nandhini Santhanam, Natascha Parks, Natasha White, Navyata Bawa, Nayan Singhal, Nick Egebo, Nicolas Usunier, Nikhil Mehta, Nikolay Pavlovich Laptev, Ning Dong, Norman Cheng, Oleg Chernoguz, Olivia Hart, Omkar Salpekar, Ozlem Kalinli, Parkin Kent, Parth Parekh, Paul Saab, Pavan Balaji, Pedro Rittner, Philip Bontrager, Pierre Roux, Piotr Dollar, Polina Zvyagina, Prashant Ratanchandani, Pritish Yuvraj, Qian Liang, Rachad Alao, Rachel Rodriguez, Rafi Ayub, Raghatham Murthy, Raghu Nayani, Rahul Mitra, Rangaprabhu Parthasarathy, Raymond Li, Rebekkah Hogan, Robin Battey, Rocky Wang, Russ Howes, Ruty Rinott, Sachin Mehta, Sachin Siby, Sai Jayesh Bondu, Samyak Datta, Sara Chugh, Sara Hunt, Sargun Dhillon, Sasha Sidorov, Satadru Pan, Saurabh Mahajan, Saurabh Verma, Seiji Yamamoto, Sharad

Ramaswamy, Shaun Lindsay, Shaun Lindsay, Sheng Feng, Shenghao Lin, Shengxin Cindy Zha, Shishir Patil, Shiva Shankar, Shuqiang Zhang, Shuqiang Zhang, Sinong Wang, Sneha Agarwal, Soji Sajuyigbe, Soumith Chintala, Stephanie Max, Stephen Chen, Steve Kehoe, Steve Satterfield, Sudarshan Govindaprasad, Sumit Gupta, Summer Deng, Sungmin Cho, Sunny Virk, Suraj Subramanian, Sy Choudhury, Sydney Goldman, Tal Remez, Tamar Glaser, Tamara Best, Thilo Koehler, Thomas Robinson, Tianhe Li, Tianjun Zhang, Tim Matthews, Timothy Chou, Tzook Shaked, Varun Vontimitta, Victoria Ajayi, Victoria Montanez, Vijai Mohan, Vinay Satish Kumar, Vishal Mangla, Vlad Ionescu, Vlad Poenaru, Vlad Tiberiu Mihailescu, Vladimir Ivanov, Wei Li, Wencheng Wang, Wenwen Jiang, Wes Bouaziz, Will Constable, Xiaocheng Tang, Xiaoqian Wu, Xiaolan Wang, Xilun Wu, Xinbo Gao, Yaniv Kleinman, Yanjun Chen, Ye Hu, Ye Jia, Ye Qi, Yenda Li, Yilin Zhang, Ying Zhang, Yossi Adi, Youngjin Nam, Yu, Wang, Yu Zhao, Yuchen Hao, Yundi Qian, Yunlu Li, Yuzi He, Zach Rait, Zachary DeVito, Zef Rosnbrick, Zhaoduo Wen, Zhenyu Yang, Zhiwei Zhao, and Zhiyu Ma. The llama 3 herd of models, 2024. URL <https://arxiv.org/abs/2407.21783>.

Suriya Gunasekar, Yi Zhang, Jyoti Aneja, Caio César Teodoro Mendes, Allie Del Giorno, Sivakanth Gopi, Mojan Javaheripi, Piero Kauffmann, Gustavo de Rosa, Olli Saarikivi, et al. Textbooks are all you need. *arXiv preprint arXiv:2306.11644*, 2023.

Dan Hendrycks and Thomas Dietterich. Benchmarking neural network robustness to common corruptions and perturbations, 2019. URL <https://arxiv.org/abs/1903.12261>.

Marius Hobbhahn, Agustinus Kristiadi, and Philipp Hennig. Fast predictive uncertainty for classification with bayesian deep networks. In *Uncertainty in Artificial Intelligence*, pages 822–832. PMLR, 2022.

Ruoxi Jia, David Dao, Boxin Wang, Frances Ann Hubis, Nezihe Merve Gurel, Bo Li, Ce Zhang, Costas J Spanos, and Dawn Song. Efficient task-specific data valuation for nearest neighbor algorithms. *arXiv preprint arXiv:1908.08619*, 2019a.

Ruoxi Jia, David Dao, Boxin Wang, Frances Ann Hubis, Nick Hynes, Nezihe Merve Gürel, Bo Li, Ce Zhang, Dawn Song, and Costas J Spanos. Towards efficient data valuation based on the shapley value. In *The 22nd International Conference on Artificial Intelligence and Statistics*, pages 1167–1176. PMLR, 2019b.

Kevin Fu Jiang, Weixin Liang, James Zou, and Yongchan Kwon. Opendataaval: a unified benchmark for data valuation. *arXiv preprint arXiv:2306.10577*, 2023.

Laurent Valentin Jospin, Hamid Laga, Farid Boussaid, Wray Buntine, and Mohammed Bennamoun. Hands-on bayesian neural networks—a tutorial for deep learning users. *IEEE Computational Intelligence Magazine*, 17(2):29–48, 2022.

Radu Jurca and Boi Faltings. Incentives for expressing opinions in online polls. In *Proceedings of the 9th ACM Conference on Electronic Commerce*, pages 119–128, 2008.

Hoang Anh Just, Feiyang Kang, Jiachen T. Wang, Yi Zeng, Myeongseob Ko, Ming Jin, and Ruoxi Jia. Lava: Data valuation without pre-specified learning algorithms, 2023. URL <https://arxiv.org/abs/2305.00054>.

Nikhil Kandpal, Eric Wallace, and Colin Raffel. Deduplicating training data mitigates privacy risks in language models. In *International Conference on Machine Learning*, pages 10697–10707. PMLR, 2022.

Pang Wei Koh and Percy Liang. Understanding black-box predictions via influence functions. In *International conference on machine learning*, pages 1885–1894. PMLR, 2017.

Yuqing Kong and Grant Schoenebeck. Equilibrium selection in information elicitation without verification via information monotonicity. In *9th Innovations in Theoretical Computer Science Conference*, 2018a.

Yuqing Kong and Grant Schoenebeck. Water from two rocks: Maximizing the mutual information. In *Proceedings of the 2018 ACM Conference on Economics and Computation*, EC ’18, page 177–194, New York, NY, USA, 2018b. Association for Computing Machinery. ISBN 9781450358293. doi: 10.1145/3219166.3219194. URL <https://doi.org/10.1145/3219166.3219194>.

Alexander Kraskov, Harald Stögbauer, and Peter Grassberger. Estimating mutual information. *Physical Review E—Statistical, Nonlinear, and Soft Matter Physics*, 69(6):066138, 2004.

Alex Krizhevsky. Learning multiple layers of features from tiny images. Technical report, University of Toronto, 2009. URL <https://www.cs.toronto.edu/~kriz/learning-features-2009-TR.pdf>.

Yongchan Kwon and James Zou. Beta shapley: a unified and noise-reduced data valuation framework for machine learning. *arXiv preprint arXiv:2110.14049*, 2021.

Yongchan Kwon, Eric Wu, Kevin Wu, and James Zou. Datainf: Efficiently estimating data influence in lora-tuned llms and diffusion models. *arXiv preprint arXiv:2310.00902*, 2023.

Kyungeun Lee and Wonjong Rhee. A benchmark suite for evaluating neural mutual information estimators on unstructured datasets. In *The Thirty-eight Conference on Neural Information Processing Systems Datasets and Benchmarks Track*, 2024.

Jeffrey Li, Alex Fang, Georgios Smyrnis, Maor Ivgi, Matt Jordan, Samir Gadre, Hritik Bansal, Etash Guha, Sedrick Keh, Kushal Arora, et al. Datacomp-lm: In search of the next generation of training sets for language models. *arXiv preprint arXiv:2406.11794*, 2024.

Yuanzhi Li, Sébastien Bubeck, Ronen Eldan, Allie Del Giorno, Suriya Gunasekar, and Yin Tat Lee. Textbooks are all you need ii: phi-1.5 technical report. *arXiv preprint arXiv:2309.05463*, 2023.

Ruizhi Liao, Daniel Moyer, Polina Golland, and William M Wells. Demi: Discriminative estimator of mutual information. *arXiv preprint arXiv:2010.01766*, 2020.

Xiaoqiang Lin, Xinyi Xu, Zhaoxuan Wu, See-Kiong Ng, and Bryan Kian Hsiang Low. Distributionally robust data valuation. In Ruslan Salakhutdinov, Zico Kolter, Katherine Heller, Adrian Weller, Nuria Oliver, Jonathan Scarlett, and Felix Berkenkamp, editors, *Proceedings of the 41st International Conference on Machine Learning*, volume 235 of *Proceedings of Machine Learning Research*, pages 30362–30391. PMLR, 21–27 Jul 2024. URL <https://proceedings.mlr.press/v235/lin24t.html>.

Xiaoqiang Lin, Xinyi Xu, See-Kiong Ng, and Bryan Kian Hsiang Low. Efficient top-m data values identification for data selection. In *The Thirteenth International Conference on Learning Representations*, 2025. URL <https://openreview.net/forum?id=10fuvmi2HT>.

Yaron Lipman, Ricky TQ Chen, Heli Ben-Hamu, Maximilian Nickel, and Matt Le. Flow matching for generative modeling. *arXiv preprint arXiv:2210.02747*, 2022.

Qian Liu, Xiaosen Zheng, Niklas Muennighoff, Guangtao Zeng, Longxu Dou, Tianyu Pang, Jing Jiang, and Min Lin. Regmix: Data mixture as regression for language model pre-training, 2025. URL <https://arxiv.org/abs/2407.01492>.

Ruibo Liu, Jerry Wei, Fangyu Liu, Chenglei Si, Yanzhe Zhang, Jinmeng Rao, Steven Zheng, Daiyi Peng, Diyi Yang, Denny Zhou, et al. Best practices and lessons learned on synthetic data for language models. *arXiv preprint arXiv:2404.07503*, 2024.

David McAllester and Karl Stratos. Formal limitations on the measurement of mutual information. In Silvia Chiappa and Roberto Calandra, editors, *Proceedings of the Twenty Third International Conference on Artificial Intelligence and Statistics*, volume 108 of *Proceedings of Machine Learning Research*, pages 875–884. PMLR, 26–28 Aug 2020. URL <https://proceedings.mlr.press/v108/mcallester20a.html>.

N. Miller, P. Resnick, and R. Zeckhauser. Eliciting informative feedback: The peer-prediction method. *Management Science*, pages 1359–1373, 2005.

Baharan Mirzasoleiman, Jeff Bilmes, and Jure Leskovec. Coresets for data-efficient training of machine learning models. In *International Conference on Machine Learning*, pages 6950–6960. PMLR, 2020.

Mohammad Mohammadi Amiri, Frederic Berdoz, and Ramesh Raskar. Fundamentals of task-agnostic data valuation. *Proceedings of the AAAI Conference on Artificial Intelligence*, 37(8):9226–9234, Jun. 2023. doi: 10.1609/aaai.v37i8.26106. URL <https://ojs.aaai.org/index.php/AAAI/article/view/26106>.

Niklas Muennighoff, Alexander Rush, Boaz Barak, Teven Le Scao, Nouamane Tazi, Aleksandra Piktus, Sampo Pyysalo, Thomas Wolf, and Colin A Raffel. Scaling data-constrained language models. *Advances in Neural Information Processing Systems*, 36, 2024.

Kevin P Murphy. *Machine learning: a probabilistic perspective*. 2012.

Frank Nielsen. On the jensen–shannon symmetrization of distances relying on abstract means. *Entropy*, 21(5):485, 2019.

Curtis Northcutt, Lu Jiang, and Isaac Chuang. Confident learning: Estimating uncertainty in dataset labels. *Journal of Artificial Intelligence Research*, 70:1373–1411, 2021.

Aaron van den Oord, Yazhe Li, and Oriol Vinyals. Representation learning with contrastive predictive coding. *arXiv preprint arXiv:1807.03748*, 2018.

Sung Min Park, Kristian Georgiev, Andrew Ilyas, Guillaume Leclerc, and Aleksander Madry. Trak: Attributing model behavior at scale. *arXiv preprint arXiv:2303.14186*, 2023.

William Peebles and Saining Xie. Scalable diffusion models with transformers. In *Proceedings of the IEEE/CVF International Conference on Computer Vision*, pages 4195–4205, 2023.

Kieu Thao Nguyen Pham, Rachael Hwee Ling Sim, Quoc Phong Nguyen, See Kiong Ng, and Bryan Kian Hsiang Low. Dupre: Data utility prediction for efficient data valuation, 2025. URL <https://arxiv.org/abs/2502.16152>.

Phillip Pope, Chen Zhu, Ahmed Abdelkader, Micah Goldblum, and Tom Goldstein. The intrinsic dimension of images and its impact on learning. *arXiv preprint arXiv:2104.08894*, 2021.

Angéline Pouget, Lucas Beyer, Emanuele Bugliarello, Xiao Wang, Andreas Peter Steiner, Xiaohua Zhai, and Ibrahim Alabdulmohsin. No filter: Cultural and socioeconomic diversityin contrastive vision-language models. *arXiv preprint arXiv:2405.13777*, 2024.

D. Prelec. A Bayesian Truth Serum for subjective data. *Science*, 306(5695):462–466, 2004.

Goran Radanovic and Boi Faltings. A robust bayesian truth serum for non-binary signals. *Proceedings of the 27th AAAI Conference on Artificial Intelligence, AAAI 2013*, 27: 833–839, 06 2013. doi: 10.1609/aaai.v27i1.8677.

Goran Radanovic and Boi Faltings. Incentives for truthful information elicitation of continuous signals. *Proceedings of the National Conference on Artificial Intelligence*, 1: 770–776, 06 2014. doi: 10.1609/aaai.v28i1.8797.

Noveen Sachdeva and Julian McAuley. Data distillation: A survey, 2023. URL <https://arxiv.org/abs/2301.04272>.

Grant Schoenebeck and Fang-Yi Yu. Learning and strongly truthful multi-task peer prediction: A variational approach, 2020a.

Grant Schoenebeck and Fang-Yi Yu. Two strongly truthful mechanisms for three heterogeneous agents answering one question. In *International Conference on Web and Internet Economics*. Springer, 2020b.

Ilia Shumailov, Zakhar Shumaylov, Yiren Zhao, Nicolas Papernot, Ross Anderson, and Yarin Gal. Ai models collapse when trained on recursively generated data. *Nature*, 631 (8022):755–759, 2024. doi: 10.1038/s41586-024-07566-y. URL <https://doi.org/10.1038/s41586-024-07566-y>.

Rachael Hwee Ling Sim, Yehong Zhang, Mun Choon Chan, and Bryan Kian Hsiang Low. Collaborative machine learning with incentive-aware model rewards. In Hal Daumé III and Aarti Singh, editors, *Proceedings of the 37th International Conference on Machine Learning*, volume 119 of *Proceedings of Machine Learning Research*, pages 8927–8936. PMLR, 13–18 Jul 2020. URL <https://proceedings.mlr.press/v119/sim20a.html>.

Jiaming Song and Stefano Ermon. Understanding the limitations of variational mutual information estimators. *arXiv preprint arXiv:1910.06222*, 2019.

Gemma Team, Thomas Mesnard, Cassidy Hardin, Robert Dadashi, Surya Bhupatiraju, Shreya Pathak, Laurent Sifre, Morgane Rivière, Mihir Sanjay Kale, Juliette Love, et al. Gemma: Open models based on gemini research and technology. *arXiv preprint arXiv:2403.08295*, 2024.

Jiachen T. Wang, Prateek Mittal, and Ruoxi Jia. Efficient data shapley for weighted nearest neighbor algorithms, 2024a. URL <https://arxiv.org/abs/2401.11103>.

Jiachen T Wang, Prateek Mittal, Dawn Song, and Ruoxi Jia. Data shapley in one training run. *arXiv preprint arXiv:2406.11011*, 2024b.

Jiachen T. Wang, Dawn Song, James Zou, Prateek Mittal, and Ruoxi Jia. Capturing the temporal dependence of training data influence, 2024c. URL <https://arxiv.org/abs/2412.09538>.

Jiachen T. Wang, Tong Wu, Dawn Song, Prateek Mittal, and Ruoxi Jia. GREATS: Online selection of high-quality data for LLM training in every iteration. In *The Thirty-eighth Annual Conference on Neural Information Processing Systems*, 2024d. URL <https://openreview.net/forum?id=232VcN8tSx>.

Jiachen T. Wang, Tianji Yang, James Zou, Yongchan Kwon, and Ruoxi Jia. Rethinking data shapley for data selection tasks: Misleads and merits, 2024e. URL <https://arxiv.org/abs/2405.03875>.

Jiachen T. Wang, Prateek Mittal, Dawn Song, and Ruoxi Jia. Data shapley in one training run. In *The Thirteenth International Conference on Learning Representations*, 2025. URL <https://openreview.net/forum?id=HD6bWcj87Y>.

Tianhao Wang and Ruoxi Jia. Data banzhaf: A data valuation framework with maximal robustness to learning stochasticity. *arXiv preprint arXiv:2205.15466*, 2022.

Yibin Wang, Haizhou Shi, Ligong Han, Dimitris Metaxas, and Hao Wang. Blob: Bayesian low-rank adaptation by backpropagation for large language models. *arXiv preprint arXiv:2406.11675*, 2024f.

Maurice Weber, Daniel Fu, Quentin Anthony, Yonatan Oren, Shane Adams, Anton Alexandrov, Xiaozhong Lyu, Huu Nguyen, Xiaozhe Yao, Virginia Adams, et al. Redpajama: an open dataset for training large language models. *arXiv preprint arXiv:2411.12372*, 2024.

Alexander Wettig, Aatmik Gupta, Saumya Malik, and Danqi Chen. Qurating: Selecting high-quality data for training language models. In *Forty-first International Conference on Machine Learning, ICML 2024, Vienna, Austria, July 21-27, 2024*. OpenReview.net, 2024. URL <https://openreview.net/forum?id=GLGYYqPwjq>.

Alexander Wettig, Kyle Lo, Sewon Min, Hannaneh Hajishirzi, Danqi Chen, and Luca Soldaini. Organize the web: Constructing domains enhances pre-training data curation. *CoRR*, abs/2502.10341, 2025. doi: 10.48550/ARXIV.2502.10341. URL <https://doi.org/10.48550/arXiv.2502.10341>.

Jens Witkowski and David C. Parkes. Peer prediction without a common prior. In Boi Faltings, Kevin Leyton-Brown, and Panos Ipeirotis, editors, *Proceedings of the 13th ACM Conference on Electronic Commerce, EC 2012, Valencia, Spain, June 4-8, 2012*, pages 964–981. ACM, 2012. doi: 10.1145/2229012.2229085. URL <https://doi.org/10.1145/2229012.2229085>.

Sang Michael Xie, Shibani Santurkar, Tengyu Ma, and Percy Liang. Data selection for language models via importance resampling, 2023. URL <https://arxiv.org/abs/2302.03169>.

Sang Michael Xie, Hieu Pham, Xuanyi Dong, Nan Du, Hanxiao Liu, Yifeng Lu, Percy S Liang, Quoc V Le, Tengyu Ma, and Adams Wei Yu. Doremi: Optimizing data mixtures speeds up language model pretraining. *Advances in Neural Information Processing Systems*, 36, 2024.

Xinnuo Xu, Minyoung Kim, Roysen Lee, Brais Martinez, and Timothy Hospedales. A bayesian approach to data point selection, 2024. URL <https://arxiv.org/abs/2411.03768>.

Xinyi Xu, Zhaoxuan Wu, Chuan Sheng Foo, and Bryan Kian Hsiang Low. Validation free and replication robust volume-based data valuation. In M. Ranzato, A. Beygelzimer, Y. Dauphin, P.S. Liang, and J. Wortman Vaughan, editors, *Advances in Neural Information Processing Systems*, volume 34, pages 10837–10848. Curran Associates, Inc., 2021. URL https://proceedings.neurips.cc/paper_files/paper/2021/file/59a3adea76fadcb6dd9e54c96fc155d1-Paper.pdf.

Adam X Yang, Maxime Robeyns, Xi Wang, and Laurence Aitchison. Bayesian low-rank adaptation for large language models. *arXiv preprint arXiv:2308.13111*, 2023.

A Blackwell ordering

We begin by providing background on the Blackwell order of information structures. We first introduce the formal definitions of decision-making problems and information structures.

Definition A.1. A decision-making problem under uncertainty is defined by the following components:

- **State Space** (Ω): A set of possible states of the world, denoted $\omega \in \Omega$.
- **Action Space** (A): A set of possible actions or decisions, denoted $a \in A$.
- **Utility Function** (u): A function $u : A \times \Omega \rightarrow \mathbb{R}$ that quantifies the payoff of taking action a in state ω .
- **Prior Belief** (P): A probability distribution over Ω , representing the decision-maker's initial beliefs. And the corresponding random variable for the state is denoted by W .

An information structure reveals some signal about the state of the world ω .

Definition A.2. An information structure S consists of a pair (\mathcal{Y}, π) , where:

- \mathcal{Y} is a set of possible signals or observations.
- $\pi : \Omega \rightarrow \Delta(\mathcal{Y})$ is a Markov kernel specifying the conditional probability $\pi(y|\omega)$ of observing signal y given state ω . The corresponding random variable representing the signal is denoted by Y .

The decision-maker observes a signal y from the information structure and updates their beliefs about the state ω using Bayes' rule. Based on the updated beliefs, they choose an action a to maximize their expected utility.

The Blackwell order provides a way to compare two information structures in terms of their informativeness, which is defined as follows.

Definition A.3 (Blackwell et al. [1951]). Let $S_1 = (\mathcal{Y}_1, \pi_1)$ and $S_2 = (\mathcal{Y}_2, \pi_2)$ be two information structures over a common state space Ω , with the corresponding signals represented by random variables Y_1 and Y_2 . We say that S_1 is *more informative* than S_2 in the Blackwell order, if there exists a Markov kernel $\kappa : \mathcal{Y}_1 \rightarrow \Delta(\mathcal{Y}_2)$ such that:

$$\pi_2(y_2|\omega) = \sum_{y_1 \in \mathcal{Y}_1} \kappa(y_2|y_1) \pi_1(y_1|\omega) \quad \forall y_2 \in \mathcal{Y}_2, \omega \in \Omega,$$

or equivalently $W \rightarrow Y_1 \rightarrow Y_2$ forms a Markov chain, where W is the random variable representing the state.

In particular, if an information structure S_1 is more informative than S_2 in the Blackwell order, then, by Blackwell's theorem on decision-making superiority, the decision-maker can achieve at least as high an expected utility using S_1 as they can using S_2 for any decision-making problem.

Theorem A.4 (Blackwell's theorem on decision-making superiority Blackwell et al. [1951]). *Let $S_1 = (\mathcal{Y}_1, \pi_1)$ and $S_2 = (\mathcal{Y}_2, \pi_2)$ be two information structures over a common state space Ω with the corresponding signals represented by random variables Y_1 and Y_2 . The following statements are equivalent:*

1. **Blackwell Informativeness:** S_1 is more informative than S_2 , or equivalently, $W \rightarrow Y_1 \rightarrow Y_2$ forms a Markov chain.
2. **Decision-Making Superiority:** For any decision-making problem (Ω, A, u, P) , the maximum expected utility achievable using S_1 is at least as high as that achievable using S_2 . Formally:

$$\max_{a_1: \mathcal{Y}_1 \rightarrow A} \mathbb{E}[u(a_1(y_1), \omega)] \geq \max_{a_2: \mathcal{Y}_2 \rightarrow A} \mathbb{E}[u(a_2(y_2), \omega)],$$

where the expectations are taken over $\omega \sim P$, $y_1 \sim \pi_1(\cdot | \omega)$, and $y_2 \sim \pi_2(\cdot | \omega)$.

We can then apply Blackwell's theorem on decision-making superiority to the problem of data valuation in machine learning. Consider the true underlying model parameter $\boldsymbol{\theta}$ as the state of the world and the dataset D as a signal about $\boldsymbol{\theta}$. Suppose we aim to use D to select a hypothesis or trained model h from a hypothesis/model class \mathcal{H} , which serves as the action space. The utility function $u(h, \boldsymbol{\theta})$ represents the negative expected loss when the true model parameter is $\boldsymbol{\theta}$ and the hypothesis/model h is chosen:

$$u(h, \boldsymbol{\theta}) = -\mathbb{E}_{\mathbf{x}, y \sim p(\mathbf{x}, y | \boldsymbol{\theta})} [l(h(\mathbf{x}), y)] \triangleq -L(h, \boldsymbol{\theta}),$$

where $l(\cdot)$ is a loss function.

Now, suppose we have a data curation strategy $f(D)$ that reduces the informativeness of the dataset D about $\boldsymbol{\theta}$ in the Blackwell order, i.e., $\boldsymbol{\theta} \rightarrow D \rightarrow f(D)$ forms a Markov chain. By Blackwell's theorem on decision-making superiority, the decision-maker can achieve at least as low an expected loss using the original dataset D as they can using the curated dataset $f(D)$.

Theorem A.5. *Let $\boldsymbol{\theta}$ be the true underlying model parameter, D_1 be a dataset consisting of data points (\mathbf{x}, y) drawn from $p(\mathbf{x}, y | \boldsymbol{\theta})$, and D_2 be a less informative dataset such that $\boldsymbol{\theta} \rightarrow D_1 \rightarrow D_2$ forms a Markov chain. Consider the decision problem of selecting a hypothesis/trained model h from a hypothesis/model class \mathcal{H} to minimize the expected loss $\mathbb{E}[l(h(\mathbf{x}), y)]$ using a dataset. Then, the minimum expected loss achievable using D_1 is at least as low as that achievable using D_2 . Formally:*

$$\min_{h_1: \mathcal{D} \rightarrow \mathcal{H}} \mathbb{E}[L(h_1(D_1), \boldsymbol{\theta})] \leq \min_{h_2: \mathcal{D} \rightarrow \mathcal{H}} \mathbb{E}[L(h_2(D_2), \boldsymbol{\theta})],$$

where $L(h, \boldsymbol{\theta}) = \mathbb{E}_{\mathbf{x}, y \sim p(\mathbf{x}, y | \boldsymbol{\theta})}[l(h(\mathbf{x}), y)]$ represents the expected loss when the true parameter is $\boldsymbol{\theta}$ and the model h is chosen. The expectation is taken over $\boldsymbol{\theta} \sim p(\boldsymbol{\theta})$, D_1 , and D_2 .

B Mutual information and proper scoring rules

Due to the data processing inequality, the simplest metric that might yield a strategy-proof scoring function is the Shannon mutual information of the model parameter $\boldsymbol{\theta}$ and the curated dataset $f(D) = \widehat{D}$, denoted by $I(\boldsymbol{\theta}, f(D))$.

One might ask whether it is possible to design a strategy-proof scoring function by estimating the mutual information $I(\boldsymbol{\theta}, f(D))$ using only $\widehat{D}_1, \dots, \widehat{D}_k$, bypassing the need for test data T . A natural approach would be to compute

$$\frac{1}{k} \sum_{i=1}^k \int_{\boldsymbol{\theta}} p(\boldsymbol{\theta} | \widehat{D}_i) \log \frac{p(\boldsymbol{\theta} | \widehat{D}_i)}{p(\boldsymbol{\theta})} d\boldsymbol{\theta} \quad (2)$$

by Monte Carlo integration, i.e., by sampling $\tilde{\boldsymbol{\theta}}$ from $p(\boldsymbol{\theta} | \widehat{D}_i)$ and compute the average $\log \frac{p(\boldsymbol{\theta} = \tilde{\boldsymbol{\theta}} | \widehat{D}_i)}{p(\boldsymbol{\theta} = \tilde{\boldsymbol{\theta}})}$.

The answer is negative. Consider the following strategic data curation method that generates a fake dataset: it converts any dataset D into a fixed dataset

$$x^* = \arg \max_{x'} \int_{\boldsymbol{\theta}} p(\boldsymbol{\theta} | D = x') \log \frac{p(\boldsymbol{\theta} | D = x')}{p(\boldsymbol{\theta})} d\boldsymbol{\theta},$$

which represents the optimal dataset x^* that maximizes the score in Equation (2). This strategic method would maximize the score computed by Equation (2), so Equation (2) does not give a strategy-proof scoring function.

To understand why Equation (2) fails and how it differs from our PMI dataset score, we introduce proper scoring rules and its connection to our problem.

Proper scoring rules. Consider the problem of designing *proper scoring rules* for probabilistic forecasts. Let Q be a forecast (represented as a probability distribution) and $S(Q, y)$ be a scoring rule that evaluates Q based on the observed true outcome y . Suppose the true distribution of y is P . A scoring rule is called *proper* if it incentivizes the forecaster to report the true distribution P , meaning:

$$\mathbb{E}_{y \sim P}[S(P, y)] \geq \mathbb{E}_{y \sim P}[S(Q, y)] \quad \text{for all } Q.$$

Equality holds if and only if $Q = P$. A well-known example of a proper scoring rule is the *logarithmic scoring rule* $S(Q, y) = \log Q(y)$, as

$$\mathbb{E}_{y \sim P}[\log P(y)] - \mathbb{E}_{y \sim P}[\log Q(y)] = D_{KL}(P \| Q) \geq 0, \quad \text{for all } Q,$$

where $D_{KL}(\cdot)$ is the KL-divergence.

However, if now we replace the true observed outcome y with a “fake” outcome $\tilde{y} \sim Q(y)$, the log scoring rule $S(Q, y) = \log Q(\tilde{y})$ will no longer be proper. As we will have the expected score

$$\mathbb{E}[S(Q, y)] = \mathbb{E} \log Q(\tilde{y}) = \mathbb{E}_{\tilde{y} \sim Q} \log Q(\tilde{y}) = -H(Q),$$

which is the negative entropy of Q and will always be maximized by a deterministic distribution.

Connection between scoring rules and our problem Our problem of evaluating data curation strategies can be viewed as a scoring rule design problem through the following mapping:

- A dataset x induces a posterior distribution over $\boldsymbol{\theta}$, which we treat as a forecast: $Q_x(\boldsymbol{\theta}) \equiv p(\boldsymbol{\theta}|D = x)$.
- A data curation strategy $f(\cdot)$ modifies this forecast to produce $Q_{f(x)}(\boldsymbol{\theta}) = p(\boldsymbol{\theta}|D = f(x))$.

So our problem can be viewed as evaluating forecasts about $\boldsymbol{\theta}$, i.e., evaluating $Q_{f(x)}(\boldsymbol{\theta}) = p(\boldsymbol{\theta}|D = f(x))$. Then computing Equation (2) by Monte Carlo integration will be equivalent to first drawing a “fake” outcome $\boldsymbol{\theta} \sim p(\boldsymbol{\theta}|D = f(x))$, and then evaluating $p(\boldsymbol{\theta}|D = f(x))$ by the fake outcome using $\log \frac{p(\boldsymbol{\theta} = \tilde{\boldsymbol{\theta}}|D = f(x))}{p(\boldsymbol{\theta} = \tilde{\boldsymbol{\theta}})}$. Then the expected score will be always be maximized by setting $f(x) \equiv x^* = \arg \max_{x'} \int p(\boldsymbol{\theta}|D = x') \log \frac{p(\boldsymbol{\theta}|D = x')}{p(\boldsymbol{\theta})} d\boldsymbol{\theta}$. This mirrors why $S(Q, y) = \log Q(\tilde{y})$ fails to be a proper scoring rule.

In contrast, our PMI dataset score can be viewed as a proper scoring rule. Let $p(\boldsymbol{\theta}, D, T)$ be the joint distribution of the true parameter and datasets. Consider the identity function $\text{id}(D) \equiv D$ and the strategic data curation method $f^*(D) \equiv x^* = \arg \max_{x'} \int_{\boldsymbol{\theta}} p(\boldsymbol{\theta}|D = x') \log \frac{p(\boldsymbol{\theta}|D = x')}{p(\boldsymbol{\theta})} d\boldsymbol{\theta}$ (here $\boldsymbol{\theta}$ can be replaced by T). By our PMI scoring function, the expected score received by $f^*(\cdot)$ is

$$S(f^*(\cdot)) = \mathbb{E}_T \left[\log \frac{p(T|D = x^*)}{p(T)} \right] = \mathbb{E}_T [\log p(T|D = x^*)] - \mathbb{E}_T \log p(T)$$

and the expected score received by $\text{id}(\cdot)$ is

$$S(\text{id}(\cdot)) = \mathbb{E}_{D, T} \left[\log \frac{p(T|D)}{p(T)} \right] = \mathbb{E}_D \mathbb{E}_{T \sim p(T|D)} [\log p(T|D)] - \mathbb{E}_T \log p(T).$$

Then we have

$$\begin{aligned} S(\text{id}(\cdot)) - S(f^*(\cdot)) &= \mathbb{E}_D \mathbb{E}_{T \sim p(T|D)} [\log p(T|D) - \log p(T|D = x^*)] \\ &= \mathbb{E}_D D_{KL}(p(T|D) \| p(T|D = x^*)) \\ &\geq 0. \end{aligned}$$

Therefore, our method properly assigns a lower score to this strategic method.

C Integral PMI score

Kong and Schoenebeck [2018b] proposes a method to compute the PMI.

Theorem C.1 (Integral PMI score [Kong and Schoenebeck, 2018b]). *The pointwise mutual information $PMI(d, t) = \log \int_{\boldsymbol{\theta}} p(\boldsymbol{\theta}|D = d)p(\boldsymbol{\theta}|T = t)/p(\boldsymbol{\theta}) d\boldsymbol{\theta}$. Therefore the data valuation function $U(d, t) = \log \int_{\boldsymbol{\theta}} p(\boldsymbol{\theta}|D = d)p(\boldsymbol{\theta}|T = t)/p(\boldsymbol{\theta}) d\boldsymbol{\theta}$ is truthful.*

Nonetheless, this integral formulation remains computationally challenging for many basic Bayesian machine learning scenarios. Chen et al. [2020b] introduced a theoretical framework for evaluating the integral score specifically within exponential family distributions; however, applying their approach is non-trivial. Computing their normalization function $g(\cdot)$ may necessitate solving a non-trivial integral.

For completeness, we provide a stand-alone proof for Theorem C.1.

Theorem C.2 (Kong and Schoenebeck [2018b], Chen et al. [2020b]). *Let D and T be two datasets that are independent conditional on $\boldsymbol{\theta}$, i.e.,*

$$p(D, T|\boldsymbol{\theta}) = p(D|\boldsymbol{\theta})p(T|\boldsymbol{\theta}),$$

then the valuation function

$$U(d, t) = \log \int_{\boldsymbol{\theta}} p(\boldsymbol{\theta}|D = d)p(\boldsymbol{\theta}|T = t)/p(\boldsymbol{\theta}) d\boldsymbol{\theta}.$$

is truthful.

Proof. This is basically because when D and T are conditionally independent, we have

$$\begin{aligned} U(d', t) &= \log \int_{\boldsymbol{\theta}} \frac{p(\boldsymbol{\theta}|D = d')p(\boldsymbol{\theta}|T = t)}{p(\boldsymbol{\theta})} d\boldsymbol{\theta} \\ &= \log \int_{\boldsymbol{\theta}} \frac{p(d'|\boldsymbol{\theta})p(t|\boldsymbol{\theta})p(\boldsymbol{\theta})}{p(d')p(t)} d\boldsymbol{\theta} \\ &= \log \frac{\int_{\boldsymbol{\theta}} p(d', t, \boldsymbol{\theta}) d\boldsymbol{\theta}}{p(d')p(t)} \\ &= \log \frac{p(d', t)}{p(d')p(t)} \\ &= \log \frac{p(t|D = d')}{p(t)} \\ &= \log p(t|D = d') - \log p(t), \end{aligned}$$

which is just the log scoring rule. If the data provider manipulates the dataset and report $f(d) = d' \neq d$, then we have

$$\begin{aligned}
& \mathbb{E}_T[U(d, T)|D = d] - \mathbb{E}_T[U(d', T)|D = d] \\
&= \sum_{t \in \mathcal{T}} p(t|D = d) \log p(t|D = d) - \sum_{t \in \mathcal{T}} p(t|D = d) \log p(t|D = d') \\
&= \sum_{t \in \mathcal{T}} p(t|D = d) \log \frac{p(t|D = d)}{p(t|D = d')} \\
&= D_{KL}(p(t|D = d), p(t|D = d')) \\
&\geq 0.
\end{aligned}$$

□

Chen et al. [2020b] proposed a theoretical framework for computing this integral score for exponential family distributions.

Definition C.3 (Exponential family Murphy [2012]). A likelihood function $p(\mathbf{x}|\boldsymbol{\theta})$, for $\mathbf{x} = (x_1, \dots, x_n) \in \mathcal{X}^n$ and $\boldsymbol{\theta} \in \Theta \subseteq \mathbb{R}^m$ is said to be in the *exponential family* in canonical form if it is of the form

$$p(\mathbf{x}|\boldsymbol{\theta}) = \frac{1}{Z(\boldsymbol{\theta})} h(\mathbf{x}) \exp [\boldsymbol{\theta}^T \boldsymbol{\phi}(\mathbf{x})] \quad \text{or} \quad p(\mathbf{x}|\boldsymbol{\theta}) = h(\mathbf{x}) \exp [\boldsymbol{\theta}^T \boldsymbol{\phi}(\mathbf{x}) - A(\boldsymbol{\theta})] \quad (3)$$

Here $\boldsymbol{\phi}(\mathbf{x}) \in \mathbb{R}^m$ is called a vector of *sufficient statistics*, $Z(\boldsymbol{\theta}) = \int_{\mathcal{X}^n} h(\mathbf{x}) \exp [\boldsymbol{\theta}^T \boldsymbol{\phi}(\mathbf{x})]$ is called the *partition function*, $A(\boldsymbol{\theta}) = \ln Z(\boldsymbol{\theta})$ is called the *log partition function*.

If the posterior distributions $p(\boldsymbol{\theta}|\mathbf{x})$ are in the same probability distribution family as the prior probability distribution $p(\boldsymbol{\theta})$, the prior and posterior are then called conjugate distributions, and the prior is called a conjugate prior.

Definition C.4 (Conjugate prior for the exponential family Murphy [2012]). For a likelihood function in the exponential family $p(\mathbf{x}|\boldsymbol{\theta}) = h(\mathbf{x}) \exp [\boldsymbol{\theta}^T \boldsymbol{\phi}(\mathbf{x}) - A(\boldsymbol{\theta})]$. The conjugate prior for $\boldsymbol{\theta}$ with parameters $\nu_0, \bar{\boldsymbol{\tau}}_0$ is of the form

$$p(\boldsymbol{\theta}) = \mathcal{P}(\boldsymbol{\theta}|\nu_0, \bar{\boldsymbol{\tau}}_0) = g(\nu_0, \bar{\boldsymbol{\tau}}_0) \exp [\nu_0 \boldsymbol{\theta}^T \bar{\boldsymbol{\tau}}_0 - \nu_0 A(\boldsymbol{\theta})]. \quad (4)$$

Let $\bar{\mathbf{s}} = \frac{1}{n} \sum_{i=1}^n \boldsymbol{\phi}(x_i)$. Then the posterior of $\boldsymbol{\theta}$ can be represented in the same form as the prior

$$p(\boldsymbol{\theta}|\mathbf{x}) \propto \exp [\boldsymbol{\theta}^T (\nu_0 \bar{\boldsymbol{\tau}}_0 + n \bar{\mathbf{s}}) - (\nu_0 + n) A(\boldsymbol{\theta})] = \mathcal{P}(\boldsymbol{\theta}|\nu_0 + n, \frac{\nu_0 \bar{\boldsymbol{\tau}}_0 + n \bar{\mathbf{s}}}{\nu_0 + n}),$$

where $\mathcal{P}(\boldsymbol{\theta}|\nu_0 + n, \frac{\nu_0 \bar{\boldsymbol{\tau}}_0 + n \bar{\mathbf{s}}}{\nu_0 + n})$ is the conjugate prior with parameters $\nu_0 + n$ and $\frac{\nu_0 \bar{\boldsymbol{\tau}}_0 + n \bar{\mathbf{s}}}{\nu_0 + n}$.

Then if the prior and the posteriors are in an exponential family, the integral PMI score can be expressed as follows using the normalization function $g(\cdot)$.

Lemma C.5. *If the model distributions are in an exponential family, so that the prior and all the posterior of $\boldsymbol{\theta}$ can be written in the form*

$$p(\boldsymbol{\theta}) = \mathcal{P}(\boldsymbol{\theta}|\nu_0, \bar{\boldsymbol{\tau}}_0) = g(\nu_0, \bar{\boldsymbol{\tau}}_0) \exp [\nu_0 \boldsymbol{\theta}^T \bar{\boldsymbol{\tau}}_0 - \nu_0 A(\boldsymbol{\theta})],$$

$p(\boldsymbol{\theta}|D) = \mathcal{P}(\boldsymbol{\theta}|\nu_D, \bar{\boldsymbol{\tau}}_D)$ and $p(\boldsymbol{\theta}|T) = \mathcal{P}(\boldsymbol{\theta}|\nu_T, \bar{\boldsymbol{\tau}}_T)$, then the pointwise mutual information can be expressed as

$$PMI(D, T) = \frac{g(\nu_D, \bar{\boldsymbol{\tau}}_D)g(\nu_T, \bar{\boldsymbol{\tau}}_T)}{g(\nu_0, \bar{\boldsymbol{\tau}}_0)g(\nu_D + \nu_T - \nu_0, \frac{\nu_D \bar{\boldsymbol{\tau}}_D + \nu_T \bar{\boldsymbol{\tau}}_T - \nu_0 \bar{\boldsymbol{\tau}}_0}{\nu_D + \nu_T - \nu_0})}.$$

However, finding the function $g(\cdot)$ is not straightforward and may involve solving a complex integral.

D Missing proofs in Section 4

D.1 Proof of Proposition 4.1

Let D and T be two datasets induced by the data generating process described in Section 3, and let $f(D)$ be any strategic data curation method so that $\boldsymbol{\theta} \rightarrow D \rightarrow f(D)$ forms a Markov chain. We want to show that the Shannon mutual information $I(f(D), T)$, if computable, is a desirable scoring function, in other words, $I(f(D), T) \leq I(D, T)$. Due to the data processing inequality, it suffices to prove that $T \rightarrow D \rightarrow f(D)$ forms a Markov chain.

Since $\boldsymbol{\theta} \rightarrow D \rightarrow f(D)$ forms a Markov chain, which means that $\boldsymbol{\theta}$ and $f(D)$ are independent conditioned on D , and D and T are independent conditioned on $\boldsymbol{\theta}$ by the data generating process, it follows that T and $f(D)$ are independent conditioned on D ,

$$\begin{aligned} & p(T, f(D)|D) \\ &= \int_{\boldsymbol{\theta}} p(T, f(D), \boldsymbol{\theta}|D) d\boldsymbol{\theta} \\ &= \int_{\boldsymbol{\theta}} p(T, f(D)|\boldsymbol{\theta}, D)p(\boldsymbol{\theta}|D) d\boldsymbol{\theta} \\ &= \int_{\boldsymbol{\theta}} p(T|f(D), \boldsymbol{\theta}, D)p(f(D)|\boldsymbol{\theta}, D)p(\boldsymbol{\theta}|D) d\boldsymbol{\theta} \\ &= \int_{\boldsymbol{\theta}} p(T|\boldsymbol{\theta})p(f(D)|D)p(\boldsymbol{\theta}|D) d\boldsymbol{\theta} \\ &= p(f(D)|D) \int_{\boldsymbol{\theta}} p(T|\boldsymbol{\theta})p(\boldsymbol{\theta}|D) d\boldsymbol{\theta} \\ &= p(f(D)|D)p(T|D). \end{aligned}$$

Therefore $T \rightarrow D \rightarrow f(D)$ forms a Markov chain as well, and by Data processing inequality, the Shannon mutual information of the curated dataset and the test dataset $I(f(D), T)$ will be a desirable scoring function if computable.

D.2 Proof of Theorem 4.2

To prove the theorem, we first prove the following lemma.

Lemma D.1. *Let D and T be two random variables that are independent conditional on random variable \mathbf{w} , that is, $p(D, T | \mathbf{w}) = p(D | \mathbf{w})p(T | \mathbf{w})$. Then we have for any $\eta \in \mathcal{W}$, $d \in \mathcal{D}$, and $t \in \mathcal{T}$,*

$$\frac{p(T = t | D = d)}{p(T = t)} = \frac{p(\mathbf{w} = \eta | D = d) \cdot p(\mathbf{w} = \eta | T = t)}{p(\mathbf{w} = \eta) \cdot p(\mathbf{w} = \eta | D = d, T = t)}.$$

The proof of Lemma D.1 mainly relies on Bayes' rule and the conditional independence condition.

Proof. Since D, T are independent conditional on \mathbf{w} , for any $\eta \in \mathcal{W}$ we have

$$\begin{aligned} & p(\mathbf{w} = \eta | D = d, T = t) \\ &= \frac{p(D = d, T = t | \mathbf{w} = \eta) \cdot p(\mathbf{w} = \eta)}{p(D = d, T = t)} \\ &= \frac{p(D = d | \mathbf{w} = \eta) \cdot p(T = t | \mathbf{w} = \eta) \cdot p(\mathbf{w} = \eta)}{p(D = d, T = t)} \\ &= \frac{p(\mathbf{w} = \eta | D = d) \cdot p(\mathbf{w} = \eta | T = t) \cdot p(D = d) \cdot p(T = t)}{p(\mathbf{w} = \eta) \cdot p(D = d, T = t)}. \end{aligned}$$

Then we have

$$\begin{aligned} \frac{p(\mathbf{w} = \eta | D = d) \cdot p(\mathbf{w} = \eta | T = t)}{p(\mathbf{w} = \eta) \cdot p(\mathbf{w} = \eta | D = d, T = t)} &= \frac{p(D = d, T = t)}{p(D = d) \cdot p(T = t)} \\ &= \frac{p(T = t | D = d)}{p(T = t)}. \end{aligned}$$

□

With this equation, we can apply the logarithmic scoring rule to get a truthful valuation function, which gives the valuation function in Theorem 4.2. The proof is as follows.

Proof. According to Lemma D.1, $U(d, t) = \log p(T = t|D = d)/P(T = t)$. Then the expected score is maximized by reporting d because

$$\begin{aligned} & \mathbb{E}_T[U_\eta(d, T)|D = d] - \mathbb{E}_T[U_\eta(d', T)|D = d] \\ &= \int_t p(t|D = d) \log p(t|D = d) dt - \int_t p(t|D = d) \log p(t|D = d') dt \\ &= \int_t p(t|D = d) \log \frac{p(t|D = d)}{p(t|D = d')} dt \\ &= D_{KL}(p(t|D = d), p(t|D = d')) \\ &\geq 0. \end{aligned}$$

And when truthful reporting, the expected score $\mathbb{E}[U_\eta(D, T)]$ is just the Shannon mutual information $I(D, T) = \mathbb{E}_{D, T} \left[\log \frac{p(D, T)}{p(D)p(T)} \right]$. \square

D.3 Proof of Corollary 4.3

We first prove that

$$\Pr \left(\left| \frac{1}{k} \sum_{i=1}^k U_\eta(\hat{D}_i, T_i) - I(\hat{D}, T) \right| \leq \varepsilon \right) \geq 1 - \delta$$

when $k = O\left(\frac{\log(1/\delta)}{\varepsilon^2}\right)$. When the posteriors belong to an exponential family and the datasets have bounded sufficient statistics, there exists a constant M such that the PMI is bounded, i.e., $U_\eta(\hat{D}_i, T_i) \leq M$. Under this condition, the concentration bound follows directly from the Chernoff bound.

The assumption of bounded sufficient statistics is similar to that in Belghazi et al. [2018b], who assume that the output of the *statistics network* is bounded (see the assumptions in their Theorem 3). The dependence on d in their bound, $O\left(\frac{d \log(\sqrt{d}/\varepsilon) + d + \log(1/\delta)}{\varepsilon^2}\right)$ mainly comes from a uniform convergence bound, which requires covering a subspace of \mathbb{R}^d with a finite number of small balls (see their proof of Theorem 6).

When the PMI is not bounded, we can still obtain a result of the same order by applying a clipping procedure. For any positive constant M , define:

$$f_M(i) = \mathbf{1}(U_\eta(\hat{D}_i, T_i) > M) \cdot U_\eta(\hat{D}_i, T_i), \quad g_M(i) = -\mathbf{1}(U_\eta(\hat{D}_i, T_i) < -M) \cdot U_\eta(\hat{D}_i, T_i).$$

Since $\mathbb{E}[U_\eta(\hat{D}_i, T_i)] = I(\hat{D}_i, T_i)$ exists (without loss of generality), the dominated convergence theorem guarantees the existence of a constant M such that:

$$\mathbb{E}[f_M(i)] \leq \varepsilon/2, \quad \mathbb{E}[g_M(i)] \leq \varepsilon/2.$$

We then clip the PMI at $\pm M$ and compute:

$$\frac{1}{k} \sum_{i=1}^k U_\eta(\hat{D}_i, T_i) \cdot \mathbf{1}(|U_\eta(\hat{D}_i, T_i)| \leq M). \quad (5)$$

This clipping introduces a bias $\in [-\varepsilon/2, \varepsilon/2]$. Furthermore, by the Chernoff bound, the clipped estimator in Equation (5) converges to its expectation within accuracy $\varepsilon/2$ with probability at least $1 - \delta$ when $k = O\left(\frac{\log(1/\delta)}{\varepsilon^2}\right)$. This completes our argument.

For the expected square error, it is equal to the variance of the estimator since the estimator is unbiased, which decrease as $O(1/k)$.

D.4 Logistic regression with Gaussian approximation

Consider logistic regression with likelihood function $p(y|\mathbf{x}, \mathbf{w}) = \text{Ber}(y|\text{Sigm}(\mathbf{w}^T \mathbf{x}))$, and consider Bayesian logistic regression with Gaussian approximation (see Murphy [2012] Chapter 8) where a Gaussian prior $p(\mathbf{w}) = \mathcal{N}(0, \Sigma_0)$ is assumed. Then given a dataset (\mathbf{X}, \mathbf{y}) , (where matrix \mathbf{X} is the input data with each column being a data feature and vector \mathbf{y} is the observed labels,) the approximate posterior is given by $p(\mathbf{w}|\mathbf{X}, \mathbf{y}) \approx \mathcal{N}(\mu, \Sigma)$ with

$$\mu = \arg \min_{\mathbf{w}} E(\mathbf{w}), \quad \Sigma^{-1} = \nabla^2 E(\mathbf{w})|\mu,$$

where $E(\mathbf{w}) = -(\log p(\mathbf{y}|\mathbf{X}, \mathbf{w}) + \log p(\mathbf{w}))$. Then μ can be solved by gradient descent and the Hessian matrix Σ^{-1} can be computed in closed form. In particular, if we pick $\Sigma_0 = \mathbf{I}$, then we have $\Sigma^{-1} = \mathbf{X}^T \mathbf{S} \mathbf{X} + \mathbf{I}$, where $\mathbf{S} = \text{diag}(\text{Sigm}(\mu^T \mathbf{x}_i)(1 - \text{Sigm}(\mu^T \mathbf{x}_i)))$. Therefore as long as the data collector knows the prior $\mathcal{N}(0, \Sigma_0)$, she will be able to compute the posterior given any dataset, and thus our PMI score can be computed by Corollary D.2. Again, we do not need to assume the distribution of the feature $p(\mathbf{x}|\mathbf{w})$ and our PMI score can be used when the test data and the evaluated data have different feature distributions.

Gaussian models. We provide the closed-form solution for the widely-used Gaussian models below. Consider a Gaussian model with a normal prior $p(\mathbf{w}) = \mathcal{N}(\mu_0, \Sigma_0)$ and normally distributed posteriors $p(\mathbf{w}|D = d) = \mathcal{N}(\mu_a, \Sigma_a)$, $p(\mathbf{w}|T = t) = \mathcal{N}(\mu_b, \Sigma_b)$, $p(\mathbf{w}|D = d, T = t) = \mathcal{N}(\mu_{ab}, \Sigma_{ab})$. We demonstrate that to compute our PMI score, it is sufficient to evaluate just two posteriors: $p(\mathbf{w}|D = d) = \mathcal{N}(\mu_a, \Sigma_a)$ and $p(\mathbf{w}|T = t) = \mathcal{N}(\mu_b, \Sigma_b)$. The parameters of the joint posterior μ_{ab}, Σ_{ab} can be derived from $\mu_a, \Sigma_a, \mu_b, \Sigma_b$. Consequently, even if data providers are unable to share the entire dataset due to privacy concerns, the PMI score can still be computed as long as the data provider submits μ_a and Σ_a .

Corollary D.2. *Suppose we have $p(\mathbf{w}|D = d) = \mathcal{N}(\mu_a, \Sigma_a)$, $p(\mathbf{w}|T = t) = \mathcal{N}(\mu_b, \Sigma_b)$, and the prior $p(\mathbf{w}) = \mathcal{N}(\mu_0, \Sigma_0)$, then our PMI score equals*

$$U_\eta(d, t) = \frac{1}{2} \left(\log \frac{\det(\Sigma_0) \det(\tilde{\Sigma})}{\det(\Sigma_a) \det(\Sigma_b)} + \mu_0^T \Sigma_0^{-1} \mu_0 + \tilde{\mu}^T \tilde{\Sigma}^{-1} \tilde{\mu} - \mu_a^T \Sigma_a^{-1} \mu_a - \mu_b^T \Sigma_b^{-1} \mu_b \right),$$

where $\tilde{\Sigma} = (\Sigma_a^{-1} + \Sigma_b^{-1} - \Sigma_0^{-1})^{-1}$ and $\tilde{\mu} = \tilde{\Sigma} (\Sigma_a^{-1} \mu_a + \Sigma_b^{-1} \mu_b - \Sigma_0^{-1} \mu_0)$. In addition, we have $p(\mathbf{w}|D=d, T=t) = \mathcal{N}(\tilde{\mu}, \tilde{\Sigma})$.

Proof. We consider Gaussian models with posteriors $p(\mathbf{w}|D=d) = \mathcal{N}(\mu_a, \Sigma_a)$, $p(\mathbf{w}|T=t) = \mathcal{N}(\mu_b, \Sigma_b)$, $p(\mathbf{w}|D=d, T=t) = \mathcal{N}(\mu_{ab}, \Sigma_{ab})$, and the prior $p(\mathbf{w}) = \mathcal{N}(\mu_0, \Sigma_0)$. Then the PMI score with $\eta = 0$ is equal to

$$U_0(d, t) = \frac{1}{2} \left(\log \frac{\det(\Sigma_0) \det(\Sigma_{ab})}{\det(\Sigma_a) \det(\Sigma_b)} + \mu_0^T \Sigma_0^{-1} \mu_0 + \mu_{ab}^T \Sigma_{ab}^{-1} \mu_{ab} - \mu_a^T \Sigma_a^{-1} \mu_a - \mu_b^T \Sigma_b^{-1} \mu_b \right). \quad (6)$$

Then it suffices to prove that $\Sigma_{ab} = (\Sigma_a^{-1} + \Sigma_b^{-1} - \Sigma_0^{-1})^{-1}$ and $\mu_{ab} = \Sigma_{ab} (\Sigma_a^{-1} \mu_a + \Sigma_b^{-1} \mu_b - \Sigma_0^{-1} \mu_0)$. Due to conditional independence and according to the proof of Lemma D.1, we have

$$\begin{aligned} p(\mathbf{w}|d, t) &\propto \frac{p(\mathbf{w}|d)p(\mathbf{w}|t)}{p(\mathbf{w})} \\ &= \frac{\mathcal{N}(\mathbf{w}; \mu_a, \Sigma_a)\mathcal{N}(\mathbf{w}; \mu_b, \Sigma_b)}{\mathcal{N}(\mathbf{w}; \mu_0, \Sigma_0)} \\ &\propto \exp \left(-\frac{1}{2} g(\mathbf{w}) \right) \end{aligned}$$

where

$$g(\mathbf{w}) := (\mathbf{w} - \mu_a)^T \Sigma_a^{-1} (\mathbf{w} - \mu_a) + (\mathbf{w} - \mu_b)^T \Sigma_b^{-1} (\mathbf{w} - \mu_b) - (\mathbf{w} - \mu_0)^T \Sigma_0^{-1} (\mathbf{w} - \mu_0)$$

Here, $g(\mathbf{w})$ can be further simplified as $g(\mathbf{w}) = (\mathbf{w} - \tilde{\mu})^T \tilde{\Sigma}^{-1} (\mathbf{w} - \tilde{\mu}) + Z_2$ where

$$\begin{aligned} \tilde{\Sigma} &= (\Sigma_a^{-1} + \Sigma_b^{-1} - \Sigma_0^{-1})^{-1} \\ \tilde{\mu} &= \tilde{\Sigma} (\Sigma_a^{-1} \mu_a + \Sigma_b^{-1} \mu_b - \Sigma_0^{-1} \mu_0) \\ Z_2 &= \mu_a^T \Sigma_a^{-1} \mu_a + \mu_b^T \Sigma_b^{-1} \mu_b - \mu_0^T \Sigma_0^{-1} \mu_0 - \tilde{\mu}^T \tilde{\Sigma}^{-1} \tilde{\mu}. \end{aligned}$$

Then $p(\mathbf{w}|d, t)$ must be the Gaussian distribution with mean $\tilde{\mu}$ and covariance matrix $\tilde{\Sigma}$. \square

E Interpretation of PMI

Our expression in Theorem 4.2 uncovers the relationship between the PMI of two datasets and the predictions they induce about \mathbf{w} . Using this expression, we demonstrate that the PMI of two datasets can be decomposed into the sum of two terms: (1) a term that measures the similarity between the outcomes obtained from two datasets, i.e., $p(\mathbf{w}|D)$ and $p(\mathbf{w}|T)$; (2) a term that measures how much D, T boost the confidence of our estimation of \mathbf{w} .

We first present the interpretation for Gaussian models and then extend it to general distributions. When the prior $p(\mathbf{w})$ is uninformative compared to $p(\mathbf{w}|d)$ and $p(\mathbf{w}|t)$, the PMI dataset score for Gaussian models can be represented as the sum of two terms: (1) a term quantifying the similarity between $p(\mathbf{w}|D)$ and $p(\mathbf{w}|T)$, characterized by the *dual skew G-Jensen-Shannon divergence* [Nielsen, 2019] between $p(\mathbf{w}|D)$ and $p(\mathbf{w}|T)$; (2) a term assessing how much D, T boost the confidence of our estimation of \mathbf{w} , which is equal to how much d and t reduce the (logarithm of the generalized) variance of our belief about \mathbf{w} .

Given two distributions p and q , the dual skew G-Jensen-Shannon divergence between p and q is their total KL divergence to their geometric mean.

Definition E.1 (Dual skew G-Jensen-Shannon divergence [Nielsen, 2019]). The dual skew G-Jensen-Shannon divergence of two distributions p, q for parameter $\alpha \in [0, 1]$ is defined as $JS_*^{G_\alpha}(p\|q) = (1-\alpha)D_{KL}(G_\alpha(p, q)\|p) + \alpha \cdot D_{KL}(G_\alpha(p, q)\|q)$, where $G_\alpha(p, q)$ is the weighted geometric mean of p and q with $G_\alpha(p, q)(x) \propto p(x)^{1-\alpha}q(x)^\alpha$.

Then the PMI dataset score can be expressed as follows.

Theorem E.2. *When the prior $p(\mathbf{w})$ is uninformative, our PMI dataset score for Gaussian models has*

$$U(d, t) = \frac{1}{2} \log \frac{|\Sigma_0|}{|\tilde{\Sigma}|} - 2 \cdot JS_*^{G_\alpha}(\mathcal{N}(\mu_a, \Sigma_a)\|\mathcal{N}(\mu_b, \Sigma_b)) - k \log 2$$

with $\alpha = 1/2$, where $\mathcal{N}(\mu_a, \Sigma_a) = p(\mathbf{w}|d)$, $\mathcal{N}(\mu_b, \Sigma_b) = p(\mathbf{w}|t)$, and $\mathcal{N}(\tilde{\mu}, \tilde{\Sigma}) = p(\mathbf{w}|d, t)$.

The negative dual skew G-Jensen-Shannon divergence indicates the similarity between $p(\mathbf{w}|D)$ and $p(\mathbf{w}|T)$. Besides the constant term $-k \log 2$, the term $\frac{1}{2} \log |\Sigma_0|/|\tilde{\Sigma}| = \frac{1}{2}(\log |\Sigma_0| - \log |\tilde{\Sigma}|)$ corresponds to the difference in (the logarithm of) the generalized variances of $p(\mathbf{w})$ and $p(\mathbf{w}|d, t)$, as the determinant of the covariance matrix is the generalized variance of a Gaussian distribution. In other words, it could be interpreted as how much d and t reduce the uncertainty or increase the confidence of our estimation. Therefore $\frac{1}{2} \log |\Sigma_0|/|\tilde{\Sigma}|$ can be interpreted as how much datasets d and t reduce uncertainty and increase confidence in our estimation.

For general distributions, if we similarly define $D_{KL}(p(\mathbf{w}|d, t)\|p(\mathbf{w}|d)) + D_{KL}(p(\mathbf{w}|d, t)\|p(\mathbf{w}|t))$ as the divergence and $D_{KL}(p(\mathbf{w}|d, t)\|p(\mathbf{w}))$ as the confidence increase, the approximation holds at equality. See Appendix E.3 for the proof and the details. In addition, this KL divergence representation can be interpreted as the “mutual information” of d and t regarding \mathbf{w} . Due to space constraints, we discuss this interpretation in Appendix E.1.

E.1 Interpretation by pointwise mutual parameter information

Firstly, our score can be represented as d and t ’s mutual information regarding \mathbf{w} , where the amount of information regarding \mathbf{w} in a dataset is measured by how much the dataset decreases the KL divergence defined below.

Definition E.3 (Pointwise parameter information of datasets). Given two datasets d, t , and a prior $p(\mathbf{w})$, define the *pointwise parameter information* of a dataset s as

$$PI_{d,t}(s) = D_{\text{KL}}(p(\mathbf{w}|d, t) \| p(\mathbf{w})) - D_{\text{KL}}(p(\mathbf{w}|d, t) \| p(\mathbf{w}|s)),$$

which represents how much observing s reduces the KL divergence to $p(\mathbf{w}|d, t)$ from our belief about \mathbf{w} . Similarly, we define the *conditional pointwise parameter information* of a dataset s given another dataset r as

$$PI_{d,t}(s|r) = D_{\text{KL}}(p(\mathbf{w}|d, t) \| p(\mathbf{w}|r)) - D_{\text{KL}}(p(\mathbf{w}|d, t) \| p(\mathbf{w}|s, r)),$$

which represents how much observing s reduces the KL divergence to $p(\mathbf{w}|d, t)$ if we have already observed r .

Then our score can be represented as “mutual information” similar to the Shannon mutual information $I(X, Y) = H(X) + H(Y) - H(X, Y) = H(X) - H(X|Y) = H(Y) - H(Y|X)$ with the entropy $H(\cdot)$ replaced by our pointwise parameter information.

Theorem E.4. *Our PMI score equals*

$$U_\eta(d, t) = PI_{d,t}(d) + PI_{d,t}(t) - PI_{d,t}(d \cup t) \triangleq PMI_{d,t}(d, t),$$

which we define as the *pointwise mutual parameter information* of d and t . In addition, we have

$$PMI_{d,t}(d, t) = PI_{d,t}(d) - PI_{d,t}(d|t) = PI_{d,t}(t) - PI_{d,t}(t|d).$$

See the proof in Appendix E.2. Theorem E.4 also suggests that our PMI score can be computed by computing/estimating KL divergence between the posteriors.

E.2 Proof of Theorem E.4

We prove the theorem by proving the following lemma.

Lemma E.5. *When D and T are independent conditional on \mathbf{w} , we have*

$$U_\eta(d, t) = D_{\text{KL}}(p(\mathbf{w}|d, t) \| p(\mathbf{w})) - D_{\text{KL}}(p(\mathbf{w}|d, t) \| p(\mathbf{w}|d)) - D_{\text{KL}}(p(\mathbf{w}|d, t) \| p(\mathbf{w}|t)).$$

Proof. The right side of the equation equals

$$\begin{aligned} & D_{\text{KL}}(p(\mathbf{w}|d, t) \| p(\mathbf{w})) - D_{\text{KL}}(p(\mathbf{w}|d, t) \| p(\mathbf{w}|d)) - D_{\text{KL}}(p(\mathbf{w}|d, t) \| p(\mathbf{w}|t)) \\ &= \int p(\mathbf{w}|d, t) \log \frac{p(\mathbf{w}|d, t)}{p(\mathbf{w})} d\mathbf{w} - \int p(\mathbf{w}|d, t) \log \frac{p(\mathbf{w}|d, t)}{p(\mathbf{w}|d)} d\mathbf{w} - \int p(\mathbf{w}|d, t) \log \frac{p(\mathbf{w}|d, t)}{p(\mathbf{w}|t)} d\mathbf{w} \\ &= \int p(\mathbf{w}|d, t) \log \frac{p(\mathbf{w}|d)p(\mathbf{w}|t)}{p(\mathbf{w}|d, t)p(\mathbf{w})} d\mathbf{w} \\ &= \log \frac{p(t|d)}{p(t)} \\ &= U_\eta(d, t). \end{aligned}$$

The third equation is due to Theorem 4.2, that is, we have $\frac{p(\mathbf{w}|d)p(\mathbf{w}|t)}{p(\mathbf{w}|d,t)p(\mathbf{w})} = \frac{p(t|d)}{p(t)}$ for all \mathbf{w} . \square

Then according to our definition of pointwise parameter information, we have

$$\begin{aligned} U_\eta(d, t) &= D_{\text{KL}}(p(\mathbf{w}|d, t)\|p(\mathbf{w})) - D_{\text{KL}}(p(\mathbf{w}|d, t)\|p(\mathbf{w}|d)) - D_{\text{KL}}(p(\mathbf{w}|d, t)\|p(\mathbf{w}|t)) \\ &= (D_{\text{KL}}(p(\mathbf{w}|d, t)\|p(\mathbf{w})) - D_{\text{KL}}(p(\mathbf{w}|d, t)\|p(\mathbf{w}|d))) \\ &\quad + (D_{\text{KL}}(p(\mathbf{w}|d, t)\|p(\mathbf{w})) - D_{\text{KL}}(p(\mathbf{w}|d, t)\|p(\mathbf{w}|t))) \\ &\quad - (D_{\text{KL}}(p(\mathbf{w}|d, t)\|p(\mathbf{w})) - D_{\text{KL}}(p(\mathbf{w}|d, t)\|p(\mathbf{w}|d, t))) \\ &= PI_{d,t}(d) + PI_{d,t}(t) - PI_{d,t}(d \cup t) \\ &\triangleq PMI_{d,t}(d, t). \end{aligned}$$

And by our definition of conditional pointwise parameter information, we have

$$\begin{aligned} U_\eta(d, t) &= (D_{\text{KL}}(p(\mathbf{w}|d, t)\|p(\mathbf{w})) - D_{\text{KL}}(p(\mathbf{w}|d, t)\|p(\mathbf{w}|d))) \\ &\quad - (D_{\text{KL}}(p(\mathbf{w}|d, t)\|p(\mathbf{w}|t)) - D_{\text{KL}}(p(\mathbf{w}|d, t)\|p(\mathbf{w}|d, t))) \\ &= PI_{d,t}(d) - PI_{d,t}(d|t). \end{aligned}$$

Similarly, we have $U_\eta(d, t) = PI_{d,t}(t) - PI_{d,t}(t|d)$.

E.3 Proof of Theorem E.2

Recall that the dual skew G-Jensen-Shannon divergence is defined as follows.

Definition E.6 (Dual skew G-Jensen-Shannon divergence [Nielsen, 2019]). The dual skew G-Jensen-Shannon divergence of two distributions p, q for parameter $\alpha \in [0, 1]$ is defined as $JS_*^{G_\alpha}(p\|q) = (1-\alpha)D_{KL}(G_\alpha(p, q)\|p) + \alpha \cdot D_{KL}(G_\alpha(p, q)\|q)$, where $G_\alpha(p, q)$ is the weighted geometric mean of p and q with $G_\alpha(p, q)(x) \propto p(x)^{1-\alpha}q(x)^\alpha$.

Nielsen [2019] solved the dual skew G-Jensen-Shannon divergence JS_*^G between two multivariate Gaussian, which is equal to the following.

Lemma E.7 (Nielsen [2019] Corollary 1). *The dual skew G-Jensen-Shannon divergence $JS_*^{G_\alpha}$ between two multivariate Gaussian $\mathcal{N}(\mu_1, \Sigma_1)$ and $\mathcal{N}(\mu_2, \Sigma_2)$ with $\alpha = \frac{1}{2}$ is equal to*

$$JS_*^{G_\alpha}(\mathcal{N}(\mu_1, \Sigma_1)\|\mathcal{N}(\mu_2, \Sigma_2)) = \frac{1}{4} \left(\mu_1^T \Sigma_1^{-1} \mu_1 + \mu_2^T \Sigma_2^{-1} \mu_2 - 2\mu^T \Sigma^{-1} \mu + \log \frac{|\Sigma_1||\Sigma_2|}{|\Sigma|^2} \right),$$

where $\Sigma = 2(\Sigma_1^{-1} + \Sigma_2^{-1})^{-1}$ and $\mu = \frac{1}{2}\Sigma(\Sigma_1^{-1}\mu_1 + \Sigma_2^{-1}\mu_2)$.

Then suppose we have $p(\mathbf{w}|D = d) = \mathcal{N}(\mu_a, \Sigma_a)$, $p(\mathbf{w}|T = t) = \mathcal{N}(\mu_b, \Sigma_b)$, the prior $p(\mathbf{w}) = \mathcal{N}(\mu_0, \Sigma_0)$, and $p(\mathbf{w}|D = d, T = t) = \mathcal{N}(\tilde{\mu}, \tilde{\Sigma})$ with $\tilde{\Sigma} = (\Sigma_a^{-1} + \Sigma_b^{-1} - \Sigma_0^{-1})^{-1} \approx$

$(\Sigma_a^{-1} + \Sigma_b^{-1})^{-1}$ and $\tilde{\mu} = \tilde{\Sigma} (\Sigma_a^{-1} \mu_a + \Sigma_b^{-1} \mu_b - \Sigma_0^{-1} \mu_0) \approx \tilde{\Sigma} (\Sigma_a^{-1} \mu_a + \Sigma_b^{-1} \mu_b)$. By definition, we have

$$JS_*^{G_\alpha}(\mathcal{N}(\mu_a, \Sigma_a) \| \mathcal{N}(\mu_b, \Sigma_b)) = \frac{1}{4} \left(\mu_a^T \Sigma_a^{-1} \mu_a + \mu_b^T \Sigma_b^{-1} \mu_b - 2\mu^T \Sigma^{-1} \mu + \log \frac{|\Sigma_a||\Sigma_b|}{|\Sigma|^2} \right),$$

where $\Sigma = 2(\Sigma_a^{-1} + \Sigma_b^{-1})^{-1} \approx 2\tilde{\Sigma}$ and $\mu = \frac{1}{2}\Sigma(\Sigma_a^{-1} \mu_a + \Sigma_b^{-1} \mu_b) \approx \tilde{\mu}$. Then $U_\eta(d, t)$ defined in Corollary D.2 has

$$\begin{aligned} U_\eta(d, t) + 2 \cdot JS_*^{G_\alpha}(\mathcal{N}(\mu_a, \Sigma_a) \| \mathcal{N}(\mu_b, \Sigma_b)) &\approx \frac{1}{2} \log \frac{\det(\Sigma_0) \det(\tilde{\Sigma})}{\det(\Sigma_a) \det(\Sigma_b)} + \frac{1}{2} \log \frac{\det(\Sigma_a) \det(\Sigma_b)}{\det(2\tilde{\Sigma})^2} \\ &= \frac{1}{2} \log \frac{\det(\Sigma_0) \det(\tilde{\Sigma})}{\det(2\tilde{\Sigma})^2} \\ &= \frac{1}{2} \log \frac{\det(\Sigma_0) \det(\tilde{\Sigma})}{4^k \cdot \det(\tilde{\Sigma})^2} \\ &= \frac{1}{2} \log \frac{\det(\Sigma_0)}{\det(\tilde{\Sigma})} - k \log 2. \end{aligned}$$

For general distributions, we can get a similar interpretation using Lemma E.5. Similar to the definition of the dual skew G-Jensen-Shannon divergence, we define $\frac{1}{2}D_{\text{KL}}(p(\mathbf{w}|d, t) \| p(\mathbf{w}|d)) + \frac{1}{2}D_{\text{KL}}(p(\mathbf{w}|d, t) \| p(\mathbf{w}|t))$ as the divergence of $p(\mathbf{w}|d)$ and $p(\mathbf{w}|t)$, where $p(\mathbf{w}|d, t)$ is viewed as the geometric mean of $p(\mathbf{w}|d)$ and $p(\mathbf{w}|t)$. In addition, we define $D_{\text{KL}}(p(\mathbf{w}|d, t) \| p(\mathbf{w}))$ as the counterpart of $\frac{1}{2} \log \frac{\det(\Sigma_0)}{\det(\tilde{\Sigma})} - k \log 2$, representing confidence increase/uncertainty reduction. Then by Lemma E.5, the PMI dataset score $U_\eta(d, t)$ equals the confidence increase $D_{\text{KL}}(p(\mathbf{w}|d, t) \| p(\mathbf{w}))$ minus the divergence $D_{\text{KL}}(p(\mathbf{w}|d, t) \| p(\mathbf{w}|d)) + D_{\text{KL}}(p(\mathbf{w}|d, t) \| p(\mathbf{w}|t))$.

F Simulations

F.1 Detailed experiment setup in Section 5.1

A benchmark for dataset MI estimation. Our benchmark generates dataset pairs with pre-defined MI values by resampling from standard datasets like MNIST and CIFAR. We construct datasets with binary labels (e.g., label 0 and 1) as follows. Given a target MI value λ , we first define a joint distribution $p(r_D, r_T)$ of two correlated numbers $r_D, r_T \in \{0.1, 0.2, \dots, 0.9\}$ such that $I(r_D, r_T) = \lambda$. Here, r_D and r_T represent the proportions of 0-labeled images in datasets D and T , respectively. Next, we sample $r_D, r_T \sim p(r_D, r_T)$ and sample images to enforce $H(r_D|D) = 0$ and $H(r_T|T) = 0$. This ensures that the ground-truth mutual information $I(D, T) = I(r_D, r_T)$. In our experiments, we generate datasets pairs with ground-truth $I(D, T) \in \{0, 0.1, \dots, 0.9, 1\}$ and assess estimation accuracy by the rank correlation between the estimated and true MI rankings.

In our setting, to establish joint probability distribution $p(r_D, r_T)$ with specified mutual information λ , we first randomly sample $a_D, a_T \in \{0.1, 0.2, 0.3, 0.4\}$ and $b_D, b_T \in \{0.6, 0.7, 0.8, 0.9\}$ independently. Then $p(r_D, r_T)$ is defined according to the structure shown in the following table, where the parameter ρ is adjusted to ensure that the mutual information $I(r_D; r_T) = \lambda$.

$p(r_D, r_T)$	$r_D = a_D$	$r_D = b_D$
$r_T = a_T$	ρ	$\frac{1}{2} - \rho$
$r_T = b_T$	$\frac{1}{2} - \rho$	ρ

We then construct dataset pairs containing images of two classes from MNIST and CIFAR. First, we randomly sample $r_D, r_T \sim p(r_D, r_T)$, which represent the proportion of data points with the label 0 in datasets D and T , respectively. Next, we generate a random vector $L_D \in \{0, 1\}^{N_D}$, where each element is 0 with probability r_D , and a similar vector $L_T \in \{0, 1\}^{N_T}$, where each element is 0 with probability r_T . Each value in L_D and L_T corresponds to a label for an image. To enforce $H(r_D|D) = 0$ and $H(r_T|T) = 0$, we make a minor modification: we replace the last bit of L_D by $\bigoplus_{j=1}^{N_D-1} L_D(i) \oplus \mathbf{1}(r_D < 0.5)$ so that the XOR sum of L_D reveals the value of r_D . Similarly, we adjust the last bit of L_T so that the XOR sum of L_T reveals r_T . Finally, we replace each label in L_D and L_T with a randomly selected image matching the label, resulting in two correlated datasets D and T .

Fact 1. *The mutual information of the generated datasets $I(D, T) = I(r_D, r_T)$.*

Proof. By Theorem 4 in [Gowri et al., 2024], $I(D, T) = I(L_D, L_T)$ assuming that $H(L_D|D) = 0$ and $H(L_T|T) = 0$. Again, since L_D and L_T fully reveals r_D and r_T , which means $H(r_D|L_D) = 0$ and $H(r_T|L_T) = 0$, Theorem 4 in [Gowri et al., 2024] implies that $I(L_D, L_T) = I(r_D, r_T)$. Therefore $I(D, T) = I(L_D, L_T) = I(r_D, r_T)$. \square

To estimate the mutual information $I(D, T) \in \{0, 0.1, \dots, 0.9, 1\}$, we generate k dataset pairs $(D_1, T_1), \dots, (D_k, T_k)$ and compute the average PMI using our formula Theorem 4.2 or other baseline methods.

Methods. To compute PMI, we employed the Bayesian logistic regression with Gaussian approximation outlined in Appendix D.4. We use the `LogisticRegression` function from the `sklearn` library. The model utilizes the L_2 norm as the regularization term, with the regularization strength controlled by C . The logistic regression model is configured with a maximum number of iterations set to 5000 (`max_iter = 5000`) and no intercept fitting (`fit_intercept = False`), while all other parameters are set to their default values. The range of C is tuned via cross-validation. We computed the estimated mutual information using our PMI formula, averaged over $k = 2000$ pairs of datasets with sizes ranging from 50 to 100. The accuracy of our approach is assessed by the Spearman's rank correlation (ρ) between the estimated mutual information rankings and the true rankings of $I(D, T)$. For

MNIST datasets, we constructed datasets by selecting images labeled as digits "0" and "1". To prevent the dimensionality of the data from being too high, we first applied Principal Component Analysis (PCA) to reduce the dimensionality to 100. For CIFAR datasets, we choose data labeled as "airplane" and "automobile". To capture image feature, we first extract image embeddings using ResNet18 pre-trained on ImageNet (with the last layer removed).

We consider the following baselines:

- **MINE:** For unstructured high-dimensional data such as images, MINE Belghazi et al. [2018b] is one of the most widely used and effective estimators for mutual information Gowri et al. [2024], Lee and Rhee [2024]. MINE has been shown to be particularly robust for image-based data, making it a strong baseline in our experiments. In our implementation, we used a three-layer neural network to estimate the mutual information, with the hidden layers having sizes of 1024 units each. The activation function used for all layers was the default ReLU function. The input to the network was formed by concatenating the raw images from the training dataset with their corresponding labels.
- **MINE on trained model parameters w :** To further reduce dimensionality, we applied MINE not directly on the raw data but on the trained logistic regression model parameters, w , which serve as a lower-dimensional proxy. The network architecture and hyperparameters used for this baseline were identical to those in the MINE implementation, with the primary difference being that the input to the neural network consisted of the parameters of the trained logistic regression model rather than the raw data.
- **LMI:** We adopt a recent approach Gowri et al. [2024], which is a method designed to estimate MI between high-dimensional variables by leveraging low-dimensional latent representations. Traditional MI estimators struggle with high-dimensional data due to the curse of dimensionality, but LMI addresses this by learning compressed representations of the variables using a cross-predictive autoencoder architecture. This architecture trains encoders and decoders to reconstruct each variable from the latent space of the other, preserving dependency structures while reducing dimensionality. Finally, alternative estimators specifically designed for low-dimensional spaces are applied to approximate MI. In our implementation, we train a four-layer neural network as encoders and decoders with LeakyReLU as activation function. The dimension of latent space is set to be 128 and we use MINE to approximate MI with low-dimension compressed representations.
- **Monte Carlo integration:** We evaluate a simple Monte Carlo integration approach to compute the pointwise mutual information defined in Proposition 4.1. The integration is computed by sampling 2000 points. First, a logistic regression model is

	CMNIST	CIFAR
PMI (C=1)	0.954 ± 0.021	-
PMI (C=100)	0.967 ± 0.015	-
PMI (C=1000)	0.961 ± 0.022	-
PMI (C=10000)	-	0.976 ± 0.000
PMI (C=20000)	-	0.976 ± 0.001
PMI (C=50000)	-	0.982 ± 0.000

Table 3: Spearman’s rank correlation (ρ) between estimated and ground-truth mutual information rankings for PMI on Colored MNIST and CIFAR. PMI consistently achieves high correlation. We sample datasets with size 100, C represents the regularization strength, and \pm denotes the standard deviation over 20 independent trials.

	CMNIST	CIFAR
PMI (C=1)	0.962 ± 0.029	-
PMI (C=100)	0.956 ± 0.024	-
PMI (C=1000)	0.964 ± 0.018	-
PMI (C=10000)	-	0.978 ± 0.001
PMI (C=20000)	-	0.984 ± 0.000
PMI (C=50000)	-	0.986 ± 0.000

Table 4: Spearman’s rank correlation (ρ) between estimated and ground-truth mutual information rankings for PMI on Colored MNIST and CIFAR. PMI achieves high correlation regardless of the regularization strength. We sample datasets with size 50, C represents the regularization strength.

trained to obtain the parameters, and then samples are drawn from both the posterior and prior distributions of these parameters. These samples are used to compute the likelihood of the test data. The Monte Carlo estimate of the likelihood is obtained by averaging the likelihoods computed for each sample. In the code, we use the log-sum-exp trick to stabilize the calculation of the logarithms of sums of exponentials. This trick is applied during the computation to avoid numerical instability by shifting the values to a more stable range before taking the logarithm, which helps in preventing overflow or underflow errors when dealing with very large or small numbers.

For each method, we perform 20 trials to compute the standard deviation of its rank correlation. We conducted our experiments on an Ubuntu system, utilizing 48GB 4090D GPUs for computations requiring GPU acceleration. Table 3, Table 4 and Figure 3 show that our PMI estimator consistently achieves high Spearman’s ρ rank correlation, producing accurate estimates with small variances under difference choices of regularization strength C and dataset sizes.

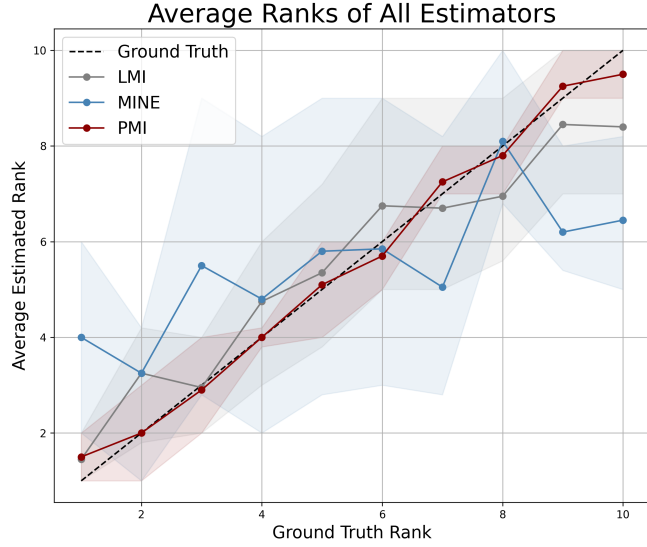


Figure 3: Estimated rankings from different methods on Colored MNIST. PMI produces the most accurate estimates with the smallest variance. The x -axis denotes the ground-truth MI ranking indices, and the y -axis denotes the estimated rankings generated by each method. The lines represent the average estimated rankings over 20 trials, while the shaded regions indicate the range of their estimations. The dataset size is 100.

F.2 Detailed experiment setup in Section 5.2

F.2.1 Colored MNIST

Experimental Settings:

In this study, we evaluate a logistic regression model with varying regularization strengths C on a colorized MNIST dataset under three scenarios: (1) Data Denoising, (2) Data Duplication, and (3) Data Removal. The training and test sets consist of samples from four categories: blue-label-0, blue-label-1, green-label-0, and green-label-1. **blue-label-0** refers to images with a blue background and a label of 0, **blue-label-1** refers to images with a blue background and a label of 1, **green-label-0** refers to images with a green background and a label of 0, and **green-label-1** refers to images with a green background and a label of 1.

The logistic regression model is implemented using the `LogisticRegression` function from the `sklearn` library. It employs the L_2 norm as the regularization term, with the strength of regularization controlled by C . The model is configured with a maximum number of iterations set to 5000 (`max_iter = 5000`) and no intercept fitting (`fit_intercept = False`),

while all other parameters are set to their default values. The range of C is tuned via cross-validation.

For each value of C , we sample 1,000 pairs of training and testing datasets. For each pair, we compute the PMI score and evaluate the model’s test accuracy by training on the training set and testing on the corresponding test set. The experiment is repeated 1,000 times for each value of C , and the mean changes in both the PMI score and test accuracy are computed. To compute the PMI score, we apply the Bayesian logistic regression with a Gaussian approximation as described in Appendix D.4. This procedure is independently repeated 10 times, resulting in 10 groups of mean values, each derived from 1,000 repetitions. From these groups, we calculate the overall mean (averaged over all 10,000 experiments) and the standard deviation (calculated across the 10 groups).

1. Data Denoising: For this scenario, we introduce noise by flipping the labels of 10 training samples prior to model training. After training, the mislabeled samples are corrected, and the model is retrained. Results are presented in Table 5 and Table 6.

2. Data Duplication: In this scenario, additional blue-label-0 and green-label-1 samples are duplicated in the training set to match the ratio of four categories of the test set. The model is retrained, and the changes in PMI Score, and Accuracy are recorded. Results are presented in Table 5 and Table 6.

3. Data Removal: Here, blue-label-0 and green-label-1 samples are removed from the training set to match the ratio of four categories of the test set. The model is retrained, and the changes in PMI Score, Loss, and Accuracy are recorded. Results are presented in Table 5 and Table 6.

F.2.2 Corrupted CIFAR

Experimental Settings. We set up the following three experiments to compare the performance of our PMI score function against the standard evaluation approach on the corrupted CIFAR dataset in evaluating three different data curation methods. We choose two classes as labels 0 and 1 among all classes in the CIFAR-10 datasets and select two corruption types (**brightness** and **contrast**) as bias in the datasets. More details of corruption design can be found in Hendrycks and Dietterich [2019].

Using the label and bias of data, we sample with different ratios in four categories: **brightness-label-0**, **contrast-label-0**, **brightness-label-1**, and **contrast-label-1**. **brightness-label-0** refers to images with **brightness** corruption and a label of 0, **contrast-label-0** refers to images with **contrast** corruption and a label of 0, **brightness-label-1** refers to images with **brightness** corruption and a label of 1, and **contrast-label-1** refers to images with **contrast** corruption and a label of 1. We sample training sets with ratio 1:1:1:1 and test sets with ratio 1:2:2:1 or 1:3:3:1 with respect to four categories.

In each experiment, we extract image embeddings using ResNet18 pre-trained on ImageNet (with the last layer removed) and flip 10% labels of the sampled training dataset to introduce noise. Then we train logistic regression models on these embeddings with

varying regularization strengths C ranging from 10000 to 100000. To further clarify, the logistic regression model is implemented using the `LogisticRegression` function from the `sklearn` library. It employs the L_2 norm as the regularization term, with the strength of regularization controlled by C . The model is configured with a maximum number of iterations set to 5000 (`max_iter = 5000`) and no intercept fitting (`fit_intercept = False`), while all other parameters are set to their default values. Here we add a dimension in embeddings where each entry is 1 and omit the bias term to integrate the bias into the weight vector. The range of C is tuned via cross-validation.

For each value of C , the experiment is repeated 1,000 times, and we compute the mean changes in PMI Score and test accuracy across these 1,000 runs. To compute our PMI we employed the Bayesian logistic regression with Gaussian approximation outlined in Appendix D.4. This process is independently repeated 10 times, producing 10 groups of mean values (each group based on 1,000 repetitions). From these 10 groups, we calculate the overall mean (averaging across all 10,000 experiments) and the standard deviation (calculated from the 10 groups of mean values). The results are summarized in Table 7 and 8.

1. Data Denoising. In this experiment, we check the change of PMI score function and test accuracy after removing the mislabeled data. We directly remove the data points whose labels are flipped.

2. Data Duplication. In this experiment, we check the change of PMI score function and test accuracy after duplicating part of training dataset to match the ratio of four categories of test dataset which is a non-essential feature irrelevant to the model.

3. Data Removal. In this experiment, we check the change of PMI score function and test accuracy after removing part of training dataset to match the ratio of four categories of test dataset which is a non-essential feature irrelevant to the model.

C	PMI Score Change	Accuracy Change(%)
Data Denoising		
10	6.4621 ± 0.8463	0.91 ± 0.06
20	6.7529 ± 0.9451	0.80 ± 0.04
50	8.1367 ± 1.0031	0.78 ± 0.11
100	12.7610 ± 1.2069	0.14 ± 0.01
200	13.5874 ± 1.0423	0.31 ± 0.02
Data Duplication		
10	-2.8150 ± 1.1563	3.84 ± 0.55
20	-1.9266 ± 1.0743	3.47 ± 0.63
50	-1.8428 ± 1.0567	3.30 ± 0.65
100	-1.8762 ± 0.9954	2.75 ± 0.54
200	-2.5927 ± 1.1437	1.43 ± 0.29
Data Removal		
10	-5.2692 ± 0.7825	0.31 ± 0.02
20	-5.1682 ± 0.8437	0.27 ± 0.02
50	-5.5265 ± 0.9823	0.28 ± 0.03
100	-6.5826 ± 1.0437	0.34 ± 0.04
200	-13.9614 ± 2.0497	0.54 ± 0.04

Table 5: **Changes** in PMI score function and test accuracy after three data curation methods with different regularization strengths **C** in the Colored MNIST dataset. The original training set, sampled from a larger dataset, consists of samples from four categories, with sizes of 50 or 100 per category, and the test set has sizes of 50, 100, 100, 50. To introduce noise, a certain percentage of the training labels are flipped. The **Denoising** method removes flipped data points, with a training set size of 50 samples per category and a test set size of 50 samples per category. The **Duplication** method adjusts the training set to match the test set’s category ratios via duplication, resulting in sizes of 50, 100, 100, 50 for the test categories. Finally, the **Removal** method reduces the training set size to match the test set category ratios, resulting in training sizes of 100, 50, 50, 100. The experiment was repeated 1,000 times to compute the mean changes in PMI scores and accuracy and repeated 10 times to compute final means and variances.

C	Change in PMI Score	Change in Accuracy (%)
Data Denoising		
10	7.8126 ± 0.9157	0.92 ± 0.08
20	7.8239 ± 1.0087	0.74 ± 0.05
50	6.2547 ± 0.9763	1.29 ± 0.09
100	14.5329 ± 1.3924	0.20 ± 0.02
200	11.9261 ± 1.1762	0.09 ± 0.02
Data Duplication		
10	-2.2345 ± 1.1247	4.50 ± 0.74
20	-1.5895 ± 1.0426	2.95 ± 0.71
50	-1.3916 ± 1.0483	3.21 ± 0.68
100	-0.4248 ± 0.2519	1.61 ± 0.54
200	-1.7580 ± 0.8914	0.97 ± 0.34
Data Removal		
10	-7.2140 ± 0.9073	0.41 ± 0.03
20	-7.5783 ± 1.1306	0.19 ± 0.01
50	-6.5111 ± 1.1430	0.21 ± 0.02
100	-7.1336 ± 0.9251	0.20 ± 0.02
200	-14.1899 ± 1.7394	0.67 ± 0.03

Table 6: **Changes** in PMI score function and test accuracy after three data curation methods with different regularization strengths **C** in the Colored MNIST dataset. The original training set, sampled from a larger dataset, consists of samples from four categories, with sizes of 50 or 150 per category, and the test set has sizes of 50, 150, 150, 50. To introduce noise, a certain percentage of the training labels are flipped. The **Denoising** method removes flipped data points, with a training set size of 50 samples per category and a test set size of 50 samples per category. The **Duplication** method adjusts the training set to match the test set’s category ratios via duplication, resulting in sizes of 50, 100, 100, 50 for the test categories. Finally, the **Removal** method reduces the training set size to match the test set category ratios, resulting in training sizes of 100, 50, 50, 100. The experiment was repeated 1,000 times to compute the mean changes in PMI scores and accuracy and repeated 10 times to compute final means and variances.

C	Change in PMI Score	Change in Accuracy (%)
Data Denoising		
10000	1.8112 \pm 0.1408	7.24 \pm 0.07
20000	1.7325 \pm 0.0916	7.21 \pm 0.11
30000	1.6553 \pm 0.1288	7.25 \pm 0.17
50000	1.5311 \pm 0.1452	7.29 \pm 0.10
100000	1.2920 \pm 0.1578	7.37 \pm 0.14
Data Duplication		
10000	-0.6288 \pm 0.0275	0.53 \pm 0.03
30000	-0.8258 \pm 0.0311	0.53 \pm 0.03
50000	-0.9025 \pm 0.0385	0.58 \pm 0.03
100000	-0.9987 \pm 0.0501	0.59 \pm 0.03
Data Removal		
10000	-3.8205 \pm 0.0892	0.69 \pm 0.07
20000	-4.1328 \pm 0.1459	0.71 \pm 0.16
30000	-4.4238 \pm 0.0847	0.77 \pm 0.10
50000	-4.6780 \pm 0.1171	0.82 \pm 0.13
100000	-5.0191 \pm 0.0969	0.79 \pm 0.16

Table 7: **Changes** in PMI score function and test accuracy after applying three data curation methods to the Corrupted CIFAR dataset. **C** denotes the regularization parameter for L2 regularization in the trained logistic regression models, corresponding to a Gaussian prior $N(0, C \cdot \mathbf{I})$. The training and the test sets consist of 120–180 samples. The experiments were repeated 1,000 times to compute the mean changes in PMI scores and test accuracy, and this process was repeated 10 times to estimate the variances. Details of the experimental setup and results for a different data distribution are provided in Appendix F.2.2.

C	Change in PMI Score	Change in Accuracy (%)
Data Denoising		
10000	2.1175 \pm 0.1916	7.38 \pm 0.11
20000	1.9854 \pm 0.1680	7.29 \pm 0.14
30000	1.9894 \pm 0.2097	7.36 \pm 0.15
50000	1.8297 \pm 0.1332	7.26 \pm 0.14
100000	1.5816 \pm 0.1717	7.31 \pm 0.09
Data Duplication		
10000	-0.2901 \pm 0.0757	0.84 \pm 0.07
20000	-0.3753 \pm 0.0793	0.86 \pm 0.06
30000	-0.5194 \pm 0.1152	0.84 \pm 0.06
50000	-0.5766 \pm 0.0758	0.86 \pm 0.06
100000	-0.8050 \pm 0.0973	0.86 \pm 0.05
Data Removal		
10000	-6.1685 \pm 0.0608	1.83 \pm 0.12
20000	-6.8668 \pm 0.1173	2.00 \pm 0.14
30000	-7.3100 \pm 0.1357	1.85 \pm 0.12
50000	-7.8402 \pm 0.1086	1.86 \pm 0.14
100000	-8.3621 \pm 0.1293	1.92 \pm 0.09

Table 8: **Changes** in PMI score function and test accuracy after three data curation methods with different regularization strengths **C** in Corrrpted CIFAR dataset. The original training set, sampled from a larger dataset, consists of images from four categories, each with size 30, and the test set has sizes 20, 60, 60, 20. To introduce noise, 10% of the training labels are flipped. The **Denoising** method simply removes flipped data points, while **Duplication** and **Removal** adjust the training set to match the test set’s category ratios via copy or delete operations, resulting in sizes of 30, 90, 90, 30 and 10, 30, 30, 10, respectively. The experiment, repeated 1,000 times to compute mean changes in PMI scores and accuracy and repeated 10 times to obtain final means and variances.